

AN EXTENSION OF THE STATISTICAL BOOTSTRAP MODEL TO INCLUDE STRANGENESS. IMPLICATIONS ON PARTICLE RATIOS

A. S. Kapoyannis, C. N. Ktorides and A. D. Panagiotou

*University of Athens, Division of Nuclear and Particle Physics,
GR-15771 Athina, Hellas*

Accepted for Publication in Physical Review D

Abstract

The Statistical Bootstrap Model (SBM) is extended to describe hadronic systems which carry the quantum number of strangeness. The study is conducted in the three-dimensional space (T, μ_q, μ_s) of temperature, up-down and strange chemical potentials, respectively, wherein the existence of a “critical” surface is established, which sets the limits of the hadronic phase of matter. A second surface, defined by the null expectation value of strangeness number ($\langle S \rangle = 0$) is also determined. The approach of the latter surface to the critical one becomes the focal point of the present considerations. Two different versions of the extended SBM are examined, corresponding to the values 2 and 4 for the exponent α , which determines the asymptotic fall-off of the mass spectrum $\rho(m)$. It is found that the $\alpha = 4$ version has decisive physical advantages. This model is subsequently adopted to discuss (strange) particle ratios pertaining to multiparticle production processes, for which a thermal equilibrium mode of description applies.

1. Introduction

The Statistical Bootstrap Model (SBM) [1,2,3] constitutes an effort for a self consistent thermodynamical description of relativistic, multiparticle systems. The basic idea is to bypass the employment of interaction between particles at a distance, in favour of successive levels of organisation of matter into particle-like entities of increasing complexity known as **fireballs**. In the context of strong interaction physics, the original set of **input** particles corresponds to all known hadrons.

The quantity which carries dynamical information in the bootstrap scheme is the mass spectrum $\rho(m)$ of the fireballs. It satisfies an integral equation with the generic form [4]:

$$\rho(m) = \delta(m - m_0) + \sum_{n=2}^{\infty} \int \frac{1}{n!} \delta \left(m - \sum_{i=1}^n m_i \right) \prod_{i=1}^n \rho(m_i) dm_i , \quad (1)$$

where m_0 represents the mass of an input particle and m_i , $i = 1, 2, \dots, \infty$, stands for the fireball masses in ascending order of complexity.

The mass spectrum determines the number of particle/fireball states, with rest- frame volume V , which reside inside the (infinitesimal) momentum region d^3p around \vec{p} , via the quantity $\frac{V}{h^3} d^3p \cdot \int \rho(m) dm$. A relativistic casting of this expression calls for the introduction of Touche's integration measure [5], as well as the adoption of a mass spectrum function $\tau(m^2)$ which depends on the relativistic invariant variable m^2 . In the system of units where $\hbar = c = k = 1$, to be adopted through this work, we write

$$\frac{V}{h^3} d^3p \cdot \int \rho(m) dm \rightarrow \frac{2V^\mu p_\mu}{2\pi^3} \int \delta_0(p^2 - m^2) d^4p \cdot \tau(m^2) dm^2 , \quad (2)$$

with $\tau(m^2)$ defined by

$$\rho(m) dm = \tau(m^2) dm^2 . \quad (3)$$

The four-volume V^μ is taken parallel to the four momentum of the particle/fireball, i.e.

$$V^\mu = \frac{V}{m} p^\mu . \quad (4)$$

Such a choice leads to the introduction of the quantity

$$B(p^2) = \frac{2V^\mu p_\mu}{(2\pi)^3} = \frac{2Vm}{(2\pi)^3} , \quad (5)$$

which will play an important role in this work, with respect to the phenomenological input entering our analysis.

The above basic features of the bootstrap scheme, when combined with a set of relations which account for statistical aspects of the system, lead to a self- consistent theoretical framework for describing the hadronic world and define the SBM. It was in the context of this approach that the idea of the existence of a critical temperature, known as Hagedorn temperature, beyond which the hadronic phase of matter ceases to maintain this self-consistent description, equivalently, ceases to exist, was first introduced [1].

An important accompanying issue raised by the above result was whether a *new* phase of matter can be realised beyond the Hagedorn temperature. Criteria have been established, within the SBM [6], which address themselves to this question and which will be explicitly referred to in the main text. Nowadays, of course, with QCD having emerged as the universally accepted microscopic theory for the strong interaction, the verdict on this matter has become clear. Lattice QCD computations [7] show that a quark gluon plasma (QGP) phase of matter should emerge under extreme conditions of high temperature and/or high density.

The intensive activity, both on the phenomenological and the experimental front, which was instigated by these non-perturbative QCD results has led to searches for the identification of specific signatures associated with the QGP state of matter. The central significance of the strangeness quantum number was soon recognised in connection with both the expected formation and subsequent hadronisation of the QGP in the ultrarelativistic nucleus-nucleus collisions.

Most theoretical attempts to study such issues approach the QGP system from the microscopic side, i.e. from a viewpoint wherein quark and gluon degrees of freedom are adopted as basic input. In the present paper we undertake a corresponding investigation from the hadronic-matter side via the employment of the SBM. We consider such an approach worth pursuing both because it should complement the theoretical attempts which originate from the microscopic side and, more importantly, because it simulates the actual experimental setting in nucleus-nucleus collisions, wherein both initial and final stages belong to the hadronic domain.

Past studies in the framework of the SBM have almost exclusively contained themselves to the non-strange hadronic sector. A first discussion of the ramifications brought onto the mass spectrum equation, cf. (1), by the inclusion of additional quantum numbers (strangeness

included) has been conducted several years ago in Ref. [8]. In the present work we undertake as our first task to systematically extend the SBM so as to create a fully thermodynamical framework which includes strangeness. This we accomplish in Section 2, where we also discuss the connection of the bootstrap scheme with QCD phenomenology, in the context of the MIT bag model [9]. We identify two cases of specific interest which are labelled by corresponding values of an exponent “ α ” that enters the asymptotic behaviour of the mass spectrum $\rho(m)$, as $m \rightarrow \infty$. The case, which has been extensively studied in the past, corresponds to $\alpha = 2$. In Section 3 we confront the analogous investigation for our extended version of the SBM, while in Section 4 we do the same for the case $\alpha = 4$. In Section 5 we present the results of our numerical study of the two versions of the strangeness incorporating SBM, which strongly advocate the case for $\alpha = 4$. On the basis of this choice we take up, in Section 6, the issue of particle production ratios for species which carry the strangeness quantum number. Taking into account the zero strangeness constraint, we present the results of numerical analyses giving particle ratios as a function of temperature T along a fixed direction in the (T, μ_q) plane, where μ_q stands for up-down chemical potential. We also provide “critical values” for these ratios, i.e. values on the intersection of the zero strangeness surface with the critical one, as functions of the critical temperature. Finally, the way to confront experimental data on particle ratios, with respect to how close they come to and/or whether they may have already reached the QGP phase, is briefly discussed. A summary of our work in this paper is presented in Section 7.

An abbreviated account of a part of the present work has been presented in a recent symposium on Strangeness in Quark Matter [10]. Here we exhibit the computational details behind our (aforementioned) contribution, as well as furnish new results pertaining to numerical procedure and particle production ratios.

2. Extension of the SBM to include strangeness

In this Section we construct an extention of the SBM which incorporates strangeness as an independent quantum number. We shall present the basic set of equations which comprise

the model, both on the bootstrap and the statistical front.

Let us begin by fixing our notational conventions with respect to particle labelling on fugacity (or chemical potential) variables. We reserve the index “a” for individual hadrons. Thus, λ_a (λ_a^{-1}) represents the fugacity of a given particle (antiparticle) belonging to the hadronic matter. Baryon number is denoted by “b”, whereas the corresponding fugacity index is “B”, i.e. we write λ_B . A similar convention is used for the, thermodynamically dual, variables pertaining to strangeness. Specifically, “S” stands for strangeness number and λ_S is the corresponding fugacity. Finally, by λ_q we denote up and down quark fugacity and by λ_s strange quark fugacity. In Table 1 we show the connection of the fugacities of the various particles we have included in our analysis with corresponding quark fugacities.

| Hadrons, a | Quark structure | Fugacity, λ_a | |
|-----------------------------------|-----------------|--------------------------------|------------------------|
| Light Unfl. Mesons | $q\bar{q}$ | $\lambda_q \lambda_q^{-1} = 1$ | Non-strange Hadrons |
| N & Δ Baryons | qqq | λ_q^3 | |
| Kaons | $q\bar{s}$ | $\lambda_q \lambda_s^{-1}$ | Strange Hadrons |
| Hyperons (Λ & Σ) | qqs | $\lambda_q^2 \lambda_s$ | |
| Ξ Baryons | qss | $\lambda_q \lambda_s^2$ | |
| Ω Baryons | sss | λ_s^3 | |

Table 1. Connection of the various hadrons with the corresponding quark fugacities.

Since the u, d quarks carry baryon number 1/3 and strangeness number 0, whereas the corresponding number for the s quark are 1/3 and -1, respectively, we have the relations

$$\lambda_q = \lambda_B^{1/3}, \quad \lambda_s = \lambda_B^{1/3} \lambda_S^{-1}, \quad (6a)$$

or, equivalently,

$$\lambda_B = \lambda_q^3, \quad \lambda_S = \lambda_q \lambda_s^{-1}. \quad (6b)$$

We now commence with the main exposition of the present Section by displaying the generic form of the bootstrap equation in the presence of strangeness. It reads as follows

(see also equ. (40) of Ref. [8]):

$$\begin{aligned} \tilde{B}(p^2)\tilde{\tau}(p^2, b, s) &= \underbrace{g_{bs}\tilde{B}(p^2)\delta_0(p^2 - m_{bs}^2)}_{\text{input term}} + \sum_{n=2}^{\infty} \frac{1}{n!} \int \delta^4 \left(p - \sum_{i=1}^n p_i \right) \cdot \\ &\cdot \sum_{\{b_i\}} \delta_K \left(b - \sum_{i=1}^n b_i \right) \sum_{\{s_i\}} \delta_K \left(s - \sum_{i=1}^n s_i \right) \prod_{i=1}^n \tilde{B}(p_i^2)\tilde{\tau}(p_i^2, b_i, s_i) d^4 p_i , \end{aligned} \quad (7)$$

where the g_{bs} represent degeneracy factors applicable to the given set of labels and where the tilde on B and τ imply a rearrangement of the form

$$B(p^2)\tau(p^2, b, s) \equiv \tilde{B}(p^2)\tilde{\tau}(p^2, b, s) \quad (8)$$

with respect to our definitions in the previous Section.

We shall refer to the first term appearing on the right hand side of (7) as **input term**, φ , and to the second as the **mass spectrum containing** term, G . The specific choice one makes in using the above relation is of crucial significance as far as the dynamical description of the SBM is concerned.

Next, we carry out three Laplace transformations, one continuous and two discrete, which lead to the replacements:

$$(p_\mu, b, s) \rightarrow (\beta_\mu, \lambda_B, \lambda_S) , \quad (9)$$

with the dual variables β_μ , λ_B , λ_S corresponding, respectively, to inverse four-temperature, baryon and strangeness fugacities. Specifically, we have

$$\begin{aligned} \varphi(\beta, \lambda_B, \lambda_S) &= \sum_{b=-\infty}^{\infty} \lambda_B^b \sum_{s=-\infty}^{\infty} \lambda_S^s \int e^{-\beta^\mu p_\mu} g_{bs}\tilde{B}(p^2)\delta_0(p^2 - m_{bs}^2) dp^4 \\ &= \frac{2\pi}{\beta} \sum_{b=-\infty}^{\infty} \lambda_B^b \sum_{s=-\infty}^{\infty} \lambda_S^s g_{bs}\tilde{B}(m_{bs}^2)m_{bs}K_1(\beta m_{bs}) \end{aligned} \quad (10)$$

for the Laplace-transformed input term and

$$\begin{aligned} G(\beta, \lambda_B, \lambda_S) &= \sum_{b=-\infty}^{\infty} \lambda_B^b \sum_{s=-\infty}^{\infty} \lambda_S^s \int e^{-\beta^\mu p_\mu} \tilde{B}(p^2)\tilde{\tau}(p^2, b, s) dp^4 \\ &= \frac{2\pi}{\beta} \int_0^\infty m\tilde{B}(m^2)\tilde{\tau}(m^2, \lambda_B, \lambda_S)K_1(\beta m) dm^2 \end{aligned} \quad (11)$$

for the Laplace-transformed mass-spectrum containing term. In the above relations K denotes the modified Bessel function of the second kind.

According to standard procedure [11] the bootstrap equation assumes the form

$$\varphi(\beta, \lambda_q, \lambda_s) = 2G(\beta, \lambda_q, \lambda_s) - \exp[G(\beta, \lambda_q, \lambda_s)] + 1 \quad (12)$$

and displays, in the $\varphi - G$ plane, a square root branch point at (see Fig. 1)

$$\varphi(T_{cr}, \mu_{q cr}, \mu_{s cr}) = \ln 4 - 1 , \quad (13a)$$

$$G(T_{cr}, \mu_{q cr}, \mu_{s cr}) = \ln 2 . \quad (13b)$$

Eq. (13a) defines a **critical surface** in the 3-d space (T, μ_q, μ_s) which sets the limits of the hadronic matter. The region radially outside the critical surface belongs to unphysical solutions of the bootstrap equation and is thereby assigned to a new phase of matter, presumably the QGP phase.

Let us also introduce the temperature T_0 according to

$$\varphi(T_0, \lambda_q = 1, \lambda_s = 1) = \ln 4 - 1 , \quad (14)$$

which constitutes the highest temperature beyond which the Hadron Gas phase does not exist.

Next, we turn our attention to the thermodynamical description of the system. According to the bootstrap scheme, the number of available states in a volume d^3p around \vec{p} , baryon number b and strangeness number s is given, in covariant form, by

$$\frac{2V_\mu^{ext} p^\mu}{(2\pi)^3} \tilde{\tau}(p^2, b, s) d^4p , \quad (15)$$

where V_μ^{ext} is the total external (four) volume available to the system. It is a constant as far as the integration over d^4p is concerned. Accordingly, the grand canonical partition function for the system reads, in covariant form,

$$\ln Z(\beta, V, \lambda_B, \lambda_S) = \sum_{b=-\infty}^{\infty} \lambda_B^b \sum_{s=-\infty}^{\infty} \lambda_S^s \int \frac{2V_\mu p^\mu}{(2\pi)^3} \tilde{\tau}(p^2, b, s) e^{-\beta^\mu p_\mu} d^4p . \quad (16)$$

Switching to quark fugacities, choosing the four-vectors V^μ and β^μ to be parallel and going to the frame for which $\beta^\mu = (\beta, 0, 0, 0)$ [11], we write

$$\ln Z(\beta, V, \lambda_q, \lambda_s) = \frac{V}{\beta 2\pi^2} \cdot \int_0^\infty m^2 \tilde{\tau}(m^2, \lambda_q, \lambda_s) K_2(\beta m) dm^2 . \quad (17)$$

Our problem now is to express the above partition function in terms of the function $G(\beta, \lambda_q, \lambda_s)$ which contains the bootstrap mass spectrum. Once this is done we shall be in position to extract specific results from the extended SBM, via the inclusion of strangeness. This we shall do in the next two Sections by referring to specific versions of our extended SBM.

We close the present Section with phenomenologically motivated remarks which will set the tone for our subsequent applications. Let us return to equation (4). The volume to mass constant provides a quantity that can be related to the MIT bag model [9]. We set

$$\frac{V}{m} = \frac{V_i}{m_i} = \frac{1}{4B} \quad , \quad (18)$$

where B is the MIT bag constant and where $V_i(m_i)$ denotes the volume (mass) of the fireball. The first equality in (18) comes from the assumption that the volume (mass) of a given fireball is the sum of the volumes (masses) of the constituent fireballs.

Let us assess the splitting between the $B(p^2)$ and $\tau(p^2, b, s)$ in the bootstrap equation. We start with the “natural” definition of $B(p^2)$ as given by (5). Here, we have a purely kinematical assignment to this quantity, so all dynamics of the bootstrap model are carried by $\tau(p^2, b, s)$ [12]. Setting $B(m^2) \equiv H_0 m^2$ we find in this case

$$H_0 = \frac{2}{(2\pi)^3 4B} \quad . \quad (19)$$

A rearrangement of the factors \tilde{B} and $\tilde{\tau}$ would imply a behaviour of the form $\tilde{B}(m^2) = \text{const} \cdot m^d$. Any choice for which $d \neq 2$ entails an absorption of part of the dynamics into \tilde{B} . Traditionally, SBM applications have centered around the choice $\tilde{B}(m^2) \sim m^0$. Setting $B(m^2) \equiv H_2$ we are now obliged to introduce a reference mass scale \tilde{m} in order to relate $\tilde{\tau}$ with τ :

$$\tilde{\tau}(m^2, b, s) = \frac{m^2}{\tilde{m}^2} \tau(m^2, b, s) \quad . \quad (20)$$

We also determine, for this case,

$$H_2 = \frac{2\tilde{m}^2}{(2\pi)^3 4B} \quad . \quad (21)$$

We stress that for any choice other than the one given by (19), one is forced to enter a reference mass scale into SBM descriptions.

Given the above remarks, relevant to the phenomenological connection with QCD, let us turn our attention to the asymptotic behaviour of the mass spectrum function $\rho(m)$, as

$m \rightarrow \infty$. It can be shown [12,13,14] that

$$\tilde{B}(m^2)\tilde{\tau}(m^2, \{\lambda\}) \xrightarrow{m \rightarrow \infty} C(\{\lambda\})m^{-3} \exp[m/T^*(\{\lambda\})] , \quad (22)$$

where $T^*(\{\lambda\})$ satisfies the criticality equation, cf. Eq. (13a). In the above relation $\{\lambda\}$ is a collective index for fugacities, while $C(\{\lambda\})$ is a quantity independent of mass.

For a given choice $\tilde{B}(m^2) = \text{const} \cdot m^d$ we have

$$\tilde{\tau}(m^2, \{\lambda\}) \xrightarrow{m \rightarrow \infty} C'(\{\lambda\})m^{-3-d} \exp[m/T^*(\{\lambda\})] ,$$

or equivalently, with reference to (3),

$$\tilde{\rho}(m^2, \{\lambda\}) \xrightarrow{m \rightarrow \infty} 2C'(\{\lambda\})m^{-\alpha} \exp[m/T^*(\{\lambda\})] , \quad (23)$$

where $\alpha = 2 + d$.

The choices, entailed by relations (19) and (21), correspond to $\alpha = 4$ and $\alpha = 2$, respectively. These two cases facilitate analytic procedures linking the grand canonical partition function to the term G , which contains the mass spectrum, and eventually, through the bootstrap equation, to the input term φ .

3. Study of the $\alpha = 2$ version of the SBM

In this section we shall study that version of the SBM which is dictated by the choice (21), equivalently $\alpha = 2$. At the hadronic level the input function is furnished by

$$\varphi(T, \lambda_q, \lambda_s) = 2\pi H_2 T \sum_a (\lambda_a + \lambda_a^{-1}) \sum_i g_{ai} m_{ai} K_1\left(\frac{m_{ai}}{T}\right) , \quad (24)$$

where the index “a” runs over all strange and non-strange hadrons. Notice that on the left hand side we have entered fugacities in terms of quark quantum numbers. The translation has to be made hadron-by-hadron according to the specifications given in the previous Section, cf. equ (6b).

The critical surface is determined by (13a), which represents a constraint among the coordinates in the 3-dimensional space $(T, \lambda_q, \lambda_s)$. The presence of the independent¹ parameter

¹In the sense that, according to (21), it can be introduced independently of the bag constant B which corresponds to a second phenomenological input parameter for the model.

H_2 in (24) allows us to use T_0 as an input to the model through the condition

$$\varphi(T_0, \lambda_q = 1, \lambda_s = 1 ; H_2) = \ln 4 - 1 , \quad (25)$$

which relates H_2 to T_0 . One can now determine the critical surface numerically for each given choice of T_0 . The relevant study will be presented in Section 5 where we shall make an assessment of our results.

Next, we turn our attention to the surface, in $(T, \lambda_q, \lambda_s)$ space, for which the expected value for the strangeness quantum number is zero. Our first task is to find a suitable expression for the grand partition function which relates it to bootstrap model quantities.

With reference to [11] let us choose a frame for which our four-volume and four-temperature are parallel to each other. If we also take the viewpoint of that inertial observer for whom $T_\mu = (T, 0, 0, 0)$, then we may write

$$\ln Z(\beta, V, \lambda_q, \lambda_s) = \frac{2V}{(2\pi)^3} \int p^0 e^{-\beta p_0} \tau_2(p^2, \lambda_q, \lambda_s) d^4 p . \quad (26)$$

We stress that in the above equation V is **not** the fireball volume, as is the case with (16), but the volume in which the thermodynamical system is enclosed. From (11) and (20) we have that

$$G(\beta, \lambda_q, \lambda_s) = H_2 \int e^{-\beta p_0} \tau_2(p^2, \lambda_q, \lambda_s) d^4 p . \quad (27)$$

Putting the last two relations together we obtain

$$\ln Z(V, \beta, \lambda_q, \lambda_s) = -\frac{2V}{(2\pi)^3 H_2} \frac{\partial}{\partial \beta} G(\beta, \lambda_q, \lambda_s) . \quad (28)$$

Referring to the bootstrap equation, (12), we easily determine

$$\frac{\partial G(\beta, \lambda_q, \lambda_s)}{\partial \beta} = \left(\frac{d\varphi}{dG} \right)^{-1} \frac{\partial \varphi(\beta, \lambda_q, \lambda_s)}{\partial \beta} = \frac{1}{2 - e^{G(\beta, \lambda_q, \lambda_s)}} \cdot \frac{\partial \varphi(\beta, \lambda_q, \lambda_s)}{\partial \beta} . \quad (29)$$

Therefore,

$$\ln Z(V, \beta, \lambda_q, \lambda_s) = -\frac{2V}{(2\pi)^3 H_2} \cdot \frac{1}{2 - e^{G(\beta, \lambda_q, \lambda_s)}} \frac{\partial \varphi(\beta, \lambda_q, \lambda_s)}{\partial \beta} . \quad (30)$$

We remark that the above equation refers to point particles. A realistic description of the system calls for volume corrections [15] which bring the bag constant B as an explicit, new input parameter. For our purposes, this procedure can be bypassed as we shall argue, *a posteriori*, shortly.

The zero strangeness condition is given by

$$\lambda_s \frac{\partial \ln Z(V, \beta, \lambda_q, \lambda_s)}{\partial \lambda_s} \bigg|_{(V, \beta, \lambda_q)} = 0 \quad (31)$$

which, with the aid of (30), becomes

$$\frac{\partial}{\partial \lambda_s} \left[\frac{1}{2 - \exp G(\beta, \lambda_q, \lambda_s)} \right] \frac{\partial \varphi(\beta, \lambda_q, \lambda_s)}{\partial \beta} + \frac{1}{2 - \exp G(\beta, \lambda_q, \lambda_s)} \frac{\partial^2 \varphi(\beta, \lambda_q, \lambda_s)}{\partial \lambda_s \partial \beta} = 0 \quad (32)$$

and finally

$$\frac{e^{G(\beta, \lambda_q, \lambda_s)}}{[2 - \exp G(\beta, \lambda_q, \lambda_s)]^2} \cdot \frac{\partial \varphi(\beta, \lambda_q, \lambda_s)}{\partial \lambda_s} \cdot \frac{\partial \varphi(\beta, \lambda_q, \lambda_s)}{\partial \beta} + \frac{\partial^2 \varphi(\beta, \lambda_q, \lambda_s)}{\partial \lambda_s \partial \beta} = 0 \quad (33)$$

The above relation specifies a surface in the three-dimensional space of $(T, \lambda_q, \lambda_s)$ onto which a hadronic system of zero strangeness must find itself. We immediately notice that the $\langle S \rangle = 0$ surface “knows” when it is approaching the critical point, i.e. a point on the critical surface since, for $G = \ln 2$, the denominator in the first factor on the rhs of (33) vanishes. This implies that the values of $(T, \lambda_q, \lambda_s)$ which lead the system to criticality are imprinted on the surface of zero strangeness.

A second characteristic of the $\langle S \rangle = 0$ contour is the fact that both strange and **non-strange** particles contribute to its specification. The presence of the non-strange particles, surviving the partial differentiation with respect to λ_s , reside in the quantities $G(\beta, \lambda_q, \lambda_s)$ and $\partial \varphi(\beta, \lambda_q, \lambda_s)/\partial \beta$. This is a significant fact, given our expectation that the critical temperature T_0 , corresponding to $\lambda_s = 1$, is of the order of the pion mass.

We finally remark that if, in the place of total strangeness, we had based our considerations on strangeness density, then we would have found

$$\langle s \rangle = \frac{\langle S \rangle}{\langle V \rangle} = \frac{\langle S \rangle}{\Delta \left(1 + \frac{\varepsilon_{pt}(\beta, \lambda_q, \lambda_s)}{4B} \right)} , \quad (34)$$

where we have taken into account the volume correction factor [15]. Accordingly, the imposition of zero strangeness density, which is enforced by the vanishing of the numerator, would lead back to (33) and our analysis would stand in its present form.

Our final undertaking of this Section is the confrontation of the problem regarding the intersection of zero-strangeness surface with the critical one, given the singular behaviour

exhibited by the former on account of the condition $G = \ln 2$. Assuming that (33) continues to hold true on the critical surface and given that the quantity $\partial^2\varphi(\beta, \lambda_q, \lambda_s)/\partial\beta\partial\lambda_s$ does not exhibit any singularity at the critical point we are led to impose the condition

$$\exp[G(\beta, \lambda_q, \lambda_s)] \cdot \frac{\partial\varphi(\beta, \lambda_q, \lambda_s)}{\partial\lambda_s} \cdot \frac{\partial\varphi(\beta, \lambda_q, \lambda_s)}{\partial\beta} \rightarrow 0 , \quad (35)$$

which, in turn, can only be satisfied if

$$\left. \frac{\partial\varphi(\beta_{cr}, \lambda_{q\,cr}, \lambda_s)}{\partial\lambda_s} \right|_{\lambda_s=\lambda_{s\,cr}} = 0 . \quad (36)$$

The above and eq. (13a) for the critical surface comprise a system of two equations that can be numerically solved and hence lead to the curve which represents the intersection of the two surfaces of interest.

The results of our numerical study of the $\langle S \rangle = 0$ surface and of its approach to the critical surface will be presented in Section 5. The next issue to occupy our attention is the consideration of the $\alpha = 4$ version of the strangeness incorporating SBM.

4. Study of the $\alpha = 4$ version of the SBM

The $\alpha = 4$ version of the SBM represents the first, integer-valued case for which the asymptotic exponent α is larger than $7/2$, namely the critical value which, in the absence of volume corrections, allows for the existence of a new phase of matter beyond the Hagedorn temperature [7]. Our relevant study will follow the patterns established in the previous Section for the $\alpha = 2$ version of the model.

The input term assumes the form

$$\varphi(T, \lambda_q, \lambda_s) = 2\pi H_0 T \sum_a (\lambda_a + \lambda_a^{-1}) \sum_i g_{ai} m_{ai}^3 K_1\left(\frac{m_{ai}}{T}\right) , \quad (37)$$

where, now, the parameter H_0 is directly related to the bag constant, cf. eq. (19). So either of the two can be considered as independent but not both. In this case, we have a direct correspondence between T_0 and B . The critical surface can now be (numerically) determined in the $(T, \lambda_q, \lambda_s)$ space, once the fugacities λ_a are adjusted to quark-related values. Results of the relevant study will be presented and discussed in the following Section.

We now proceed to consider the zero strangeness surface. We start by determining the form acquired by the bootstrap function G for the case in hand. We find

$$\begin{aligned} G(\beta, \lambda_q, \lambda_s) &= \frac{2\pi}{\beta} \int_0^\infty m B_0(m^2) \tau_0(m^2, \lambda_q, \lambda_s) K_1(\beta m) dm^2 \\ &= \frac{2\pi H_0}{\beta} \int_0^\infty m^3 \tau_0(m^2, \lambda_q, \lambda_s) K_1(\beta m) dm^2 \quad . \end{aligned} \quad (38)$$

We shall use the relation

$$\frac{d}{d\beta} [\beta^2 K_2(m\beta)] = -m\beta^2 K_1(m\beta) \quad , \quad (39)$$

which follows from the Bessel function identities $K_{n+1}(x) = \left(\frac{2n}{x}\right) K_n(x) + K_{n-1}(x)$ and $K'_n(x) = -\frac{1}{2}[K_{n+1}(x) + K_{n-1}(x)]$. Further, taking into account the asymptotic property

$$\lim_{x \rightarrow \infty} x^2 K_2(mx) = \lim_{x \rightarrow \infty} \sqrt{\frac{\pi}{2}} x^{3/2} e^{-x} = 0 \quad (40)$$

the logarithm of the grand canonical partition function (17) becomes

$$\ln Z(\beta, V, \lambda_q, \lambda_s) = \frac{V}{\beta^3 2\pi^2} \cdot \int_0^\infty m^2 \tau_0(m^2, \lambda_q, \lambda_s) \left\{ \int_\infty^\beta \frac{d}{dx} [x^2 K_2(xm)] dx \right\} dm^2 \quad . \quad (41)$$

Use of (39) and (38) finally gives

$$\ln Z(\beta, V, \lambda_q, \lambda_s) = \frac{V}{4\pi^3 H_0} \frac{1}{\beta^3} \int_\beta^\infty x^3 G(x, \lambda_q, \lambda_s) dx \quad . \quad (42)$$

The zero strangeness condition now translates into

$$\int_\beta^\infty x^3 \frac{\partial G(x, \lambda_q, \lambda_s)}{\partial \lambda_s} dx = 0 \quad . \quad (43)$$

With the aid of the bootstrap equation, relation (43) becomes

$$\int_\beta^\infty x^3 \frac{1}{2 - \exp[G(x, \lambda_q, \lambda_s)]} \frac{\partial \varphi(x, \lambda_q, \lambda_s)}{\partial \lambda_s} dx = 0 \quad . \quad (44)$$

Making the variable change $x=1/y$, the above relation takes the form

$$\int_0^T \frac{1}{y^5} \frac{1}{2 - \exp[G(y, \lambda_q, \lambda_s)]} \frac{\partial \varphi(y, \lambda_q, \lambda_s)}{\partial \lambda_s} dy = 0 \quad , \quad (45)$$

which is well defined, having no problems at $y = 0$ despite the presence of the factor y^{-5} . The point is that $\varphi(y, \lambda_q, \lambda_s)$ carries with it terms containing the Bessel function $K_1(m/y)$

which is not affected by the partial differentiation with respect to λ_s . But, the argument of the K_1 functions tends to infinity as $y \rightarrow 0$, which leads to $\lim_{y \rightarrow 0} y^{-5} K_1(m/y) = 0$. On the other hand, the problem associated with the approach to the critical point, at $G = \ln 2$, persists as with the $\alpha = 2$ version of the previous Section. So, even if the integral is well defined, we shall have to face tedious convergence problems during the course of a numerical analysis which aims at determining the intersection of the $\langle S \rangle = 0$ with the critical surface.

We bypass the aforementioned problem by introducing a new variable, as follows. Setting

$$z = 2 - \exp[G(y, \lambda_q, \lambda_s)] , \quad (46)$$

we determine

$$dz = -\frac{e^G}{2 - e^G} \frac{\partial \varphi(y, \lambda_q, \lambda_s)}{\partial y} dy . \quad (47)$$

From (46) it also follows that $-e^G = z - 2$, whereupon we conclude

$$\frac{dy}{2 - \exp[G(\beta, \lambda_q, \lambda_s)]} = \frac{dz}{z - 2} \left\{ \left[\frac{\partial \varphi(y, \lambda_q, \lambda_s)}{\partial y} \right]^{-1} \right\} \Big|_{z = 2 - \exp[G(y, \lambda_{q\,cr}, \lambda_{s\,cr})]} . \quad (48)$$

Next, we must determine the limits for the dz integration. We assume that the fugacities λ_q and λ_s remain finite as $y \rightarrow 0$. But then, the bootstrap equation, along with the fact that $\lim_{y \rightarrow 0} \varphi(y, \lambda_q, \lambda_s) = 0$, gives $z = 2 - e^0 = 1$. For the upper limit, the real interest lies with T approaching a critical value. At this point we have $z = 2 - e^{\ln 2} = 0$. We, therefore, obtain

$$\int_1^0 \frac{dz}{z - 2} \cdot \left[\frac{\frac{\partial \varphi(y, \lambda_{q\,cr}, \lambda_{s\,cr})}{\partial \lambda_s}}{y^5 \cdot \frac{\partial \varphi(y, \lambda_{q\,cr}, \lambda_{s\,cr})}{\partial y}} \right]_{z = 2 - \exp[G(y, \lambda_{q\,cr}, \lambda_{s\,cr})]} = 0 . \quad (49)$$

Notice that at the critical point, where $z = 0$, no singularity appears, which explicitly shows that the (apparent) singularity at $G = \ln 2$ is integrable.

As it turns out, the z -variable is favoured with respect to convergence properties at the upper limit, i.e when one is approaching a critical surface value, whereas the y -integration is more efficiently performed at the lower limit. The best of both cases is attained by introducing an intermediate temperature \tilde{T} , conveniently chosen so that the function which is integrated vanishes at this temperature, and determine $\langle S \rangle = 0$ surface via the equation

$$\begin{aligned}
& \int_0^{\tilde{T}} \frac{1}{2 - \exp[G(y, \lambda_{q cr}, \lambda_{s cr})]} \frac{\partial \varphi(y, \lambda_{q cr}, \lambda_{s cr})}{\partial \lambda_s} \frac{dy}{y^5} + \\
& \int_{\tilde{z}}^0 \frac{dz}{z - 2} \cdot \left[\frac{\frac{\partial \varphi(y, \lambda_{q cr}, \lambda_{s cr})}{\partial \lambda_s}}{y^5 \cdot \frac{\partial \varphi(y, \lambda_{q cr}, \lambda_{s cr})}{\partial y}} \right]_{z=2-\exp[G(y, \lambda_{q cr}, \lambda_{s cr})]} = 0 . \quad (50)
\end{aligned}$$

Our specification for \tilde{T} is fulfilled if it is determined by the relation

$$\left. \frac{\partial \varphi(\tilde{T}, \lambda_{q cr}, \lambda_s)}{\partial \lambda_s} \right|_{\lambda_s=\lambda_{s cr}} = 0 \quad (51)$$

according to which the lower limit of the dz -integration in (50) is

$$\tilde{z} = 2 - \exp[G(\tilde{T}, \lambda_{q cr}, \lambda_{s cr})] . \quad (52)$$

In the next Section we shall present the results of our numerical investigation of the $\alpha = 4$ version of the SBM and argue in favour of its suitability over the $\alpha = 2$ version, as far as its implications near the critical surface are concerned.

5. Behaviour near the Critical Surface

In this Section we present the results of our numerical calculations of the critical and zero-strangeness surfaces in the (T, μ_q, μ_s) three-dimensional space of the two versions of the SBM discussed in the previous sections. Specifically, we shall study the corresponding behaviours of the $\alpha = 2$ and $\alpha = 4$ cases as one approaches the critical surface, which, in the SBM context, signifies the termination of the hadronic world. Notice that we have chosen chemical potential variables in terms of which to present our findings, instead of fugacities.

5.1. $\alpha = 2$ case

Let us begin with the critical surface for the case of $\alpha = 2$. Choosing as input value 180 MeV for the T_0 variable, we depict, in figures 2a,b, two different profiles of the aforementioned surface. Fig. 2a shows that for a range of values of μ_s in the interval $[0, 100]$ MeV, the critical surface is virtually perpendicular to the $T - \mu_q$ plane. This indicates that, for a system in

this range of μ_s values, the critical surface is basically determined by T and μ_q . One also notices that the curves corresponding to constant μ_s converge to a value of about 330 MeV for μ_q , as $T \rightarrow 0$, whilst (Fig. 2b) curves of constant μ_q , in the same limit and on the positive side, towards $\mu_s \simeq 560$ MeV.

The dependence of the critical surface on the input parameter T_0 , is the object of attention in figures 3a,b. We depict characteristic intersections of the $\mu_s = 0$ and $\mu_q = 0$ planes, respectively, by the critical surface, for different values of T_0 . We notice that towards low temperatures the dependence on T_0 is very slight. One must keep in mind, however, that this is the least trustworthy region of our analysis, since the Boltzmann approximation is rather inadequate for low temperatures.

Turning our attention to the $\langle S \rangle \geq 0$ surface we choose a fixed value for the ratio μ_q/T , 0.4 to be specific, and study the variation of μ_s with temperature. The result of the relevant numerical study is shown in figure 4 for various values of T_0 . The vertical lines in the figure show the edge of the cylindrical, critical surface corresponding to the same value of the μ_q/T ratio, in the vicinity of small values for the μ_s chemical potential. Finally, the uninterrupted curve represents the zero strangeness contour, for $\mu_q/T = 0.4$, which results from an “ideal hadron gas” analysis [16,17] wherein the bootstrap equation does not provide an input to the partition function. It is satisfying to witness an agreement between the two descriptions up to a certain point. The observed tendency is for the bootstrap description to drive towards higher values for μ_s as the critical surface is approached². At a given point the chemical potential μ_s reverses its course and merges with the critical surface on its way up. Finally, in the same figure we exhibit an extreme case, corresponding to $T_0 = 250$ MeV, for which the $\langle S \rangle \geq 0$ surface dips into the negative value region for the strange chemical potential before merging with the critical surface.

In figures 5a,b we depict the profile of the intersection curve between the $\langle S \rangle \geq 0$ and critical surfaces for $\alpha = 2$, by projecting it on the $(\mu_{q\,cr}, \mu_{s\,cr})$ and $(T, \mu_{s\,cr})$ planes, respectively, for various values of T_0 . Note that there exists a value for T_0 , equal to about 232 MeV, for which the intersection curve stays for long distance in touch with $\mu_{s\,cr} = 0$. For smaller values of T_0 , the $(\mu_{q\,cr}, \mu_{s\,cr})$ dependence along the intersection curve is monotonous,

²In the “ideal hadron gas” model, of course, there is no critical surface.

while below the aforementioned value, it dips into the negative $\mu_{s\ cr}$ range before rising up.

5.2. $\alpha = 4$ case

We now turn our attention to the $\alpha = 4$ version of the SBM which has received minimal attention in the past. The present incorporation of strangeness into the bootstrap scheme will bring out decisive advantages of this over the $\alpha = 2$ case, which has dominated SBM studies up to now.

The numerical study of the $\alpha = 4$ case is quite demanding, certainly more so than its $\alpha = 2$ counterpart. It might be helpful to briefly remark on the procedure employed for the determination of the $\langle S \rangle = 0$ surface, for $\alpha = 4$. Starting from (45) we give input values to the quantities (λ_q, T) and compute the λ_s value for which the left hand side vanishes. We use the Newton-Raphson method which also requires knowledge of the first derivative of the function. The latter is given by

$$\int_0^T \frac{dy}{y^5} \left\{ \frac{\exp[G(y, \lambda_q, \lambda_s)]}{\{2 - \exp[G(y, \lambda_q, \lambda_s)]\}^3} \left[\frac{\partial \varphi(y, \lambda_q, \lambda_s)}{\partial \lambda_s} \right]^2 + \right. \\ \left. + \frac{1}{2 - \exp[G(y, \lambda_q, \lambda_s)]} \frac{\partial^2 \varphi(y, \lambda_q, \lambda_s)}{\partial \lambda_s^2} \right\} = 0 . \quad (53)$$

The integration in (45) is performed via appropriate routines.

For temperatures which approach the critical one, i.e. $T^*(\lambda_{q\ cr}, \lambda_{s\ cr})$, computations are facilitated by employing the transformation $w = (T^* - y)^{1/2}$. To see this observe that the encountered singularity is of the form $(2 - e^G)^{-1}$, equivalently, via the use of the bootstrap equation, $\frac{1}{2}(\varphi_0 - \varphi)^{-1/2}$. But, then, a Taylor expansion of φ around T^* ,

$$\varphi_0 - \varphi(y, \lambda_q, \lambda_s) \approx C[T^*(\lambda_{q\ cr}, \lambda_{s\ cr})][T^*(\lambda_{q\ cr}, \lambda_{s\ cr}) - y] , \quad (54)$$

ascertains that the aforementioned transformation does away with the singularity.

Not knowing T^* *a priori*, use of the w variable gives satisfactory results for values of T in the vicinity of T^* but not for $T = T^*$. The problem is confronted by appealing to (50). Using as input a critical value for the up-down quark fugacity, $\lambda_q = \lambda_{q\ cr}$, we determine the corresponding value for $\lambda_{s\ cr}$. We do not use the Newton-Raphson method for extracting $\lambda_{q\ cr}$ given the complex expression entering the left hand side of (50). Instead, we employ the “Brent” method which furnishes a value for the root once we specify an interval

wherein the said root lies. Finally, T^* is determined via a numerical solution of the equation $\varphi(T^*, \lambda_q, \lambda_s) = \ln 4 - 1$.

Figures 6-10 summarise the findings of our numerical investigations for the $\alpha = 4$ version of the extended SBM. In figures 6a,b we depict the profile of the critical surface in a similar manner as done for the $\alpha = 2$ case in figures 2a,b. The critical surface does not depend appreciably on μ_s for an extended range of values on either side of the $\mu_s = 0$ (Fig. 6b illustrates this occurrence only for positive values of μ_q). Near $T = 0$ the critical surface converges towards $\mu_q \approx 325$ MeV for $\mu_s = 0$ (Fig. 6a) and $\mu_s \approx 550$ MeV for $\mu_q = 0$ (Fig. 6b). In figures 7a,b we exhibit intersections of the critical surface for different values of T_0 , just as figures 3a,b show for the $\alpha = 2$ case.

A comparative study between the $\alpha = 2$ and $\alpha = 4$ versions of the SBM is presented in figures 8a,b. Here, for the fixed value of 180 MeV for T_0 , we show the intersections of the critical surface with the planes (T, μ_q) and (T, μ_s) , respectively, as well as a second, parallel intersection. One witnesses a similar behaviour of the two cases.

The numerical study of the $\langle S \rangle = 0$ surface for the SBM choice $\alpha = 4$, though much harder, *can* be achieved. As with the $\alpha = 2$ case, we present, in figure 9, curves on the zero strangeness surface displaying the $T - \mu_s$ dependence for the constant ratio $\mu_q/T = 0.4$ and for different values of T_0 . As before, the (almost) vertical lines represent the critical surface and adhere to the same μ_q/T ratio. We note that the curves $\mu_s(T)$ on $\langle S \rangle = 0$ approach tangentially the critical surface, without reversing their course. Notice the remarkable coincidence with the “ideal hadron gas” model curve up to a temperature which is only 25 MeV, or so, away from the critical surface.

Figures 10a,b are analogous to figures 5a,b, respectively, for the $\alpha = 2$ case. We observe a similar behaviour of the intersection of the surface $\langle S \rangle = 0$ with the critical surface. But, note that the value of T_0 for which the intersection curve stays for long distance in touch with $\mu_s^{cr} = 0$, is now much smaller (and more realistic) and equals 183 MeV. Finally, in figure 11 we give a three-dimensional plot in the (T, μ_q, μ_s) space for $T_0 = 183$ MeV. We display different cuts of the surface of zero strangeness, which correspond to constant fugacity λ_q , fixed by the ratio μ_q/T . On the same plot we also present the intersection of the zero-strangeness surface with the critical surface.

5.3. Relative Assessments - Prevalence of the $\alpha = 4$ version

Let us proceed with an evaluation of our present findings, starting with the $\alpha = 2$ version of the strangeness including SBM. The sudden upward trend of the chemical potential μ_s is an unwelcome occurrence, despite the agreement with the “ideal hadron gas” analysis, prior to approaching criticality. Indeed, our expectation that a QGP state of matter lying beyond the critical point would imply a tendency of μ_s towards zero and not away from it. Even if there exists an intermediate phase between the hadronic and the QGP states, which interpolates between constituent and current quarks, one would still expect μ_s in this phase to be smaller than in the pure hadronic one. Therefore we fully expect μ_s to **converge** towards zero as criticality is approached and not to move away from it.

A second point of discouragement has to do with particle ratios, for which a more detailed discussion will be conducted in the next section. Let us take, for example, the $\bar{\Xi}/\Xi$ ratio. In the “ideal hadron gas” model it is a genuinely monotonic increasing function of temperature. This is a trend we expect to be enhanced, as the (assumed) QGP phase is reached. Unfortunately, within the framework of the $\alpha = 2$ version of the SBM we find this ratio to go down with temperature, as the critical point is approached.

On a purely theoretical basis it is especially bothersome that volume correction ramifications seem to have no impact on our $\alpha = 2$ analysis³. Given that such corrections are integrally connected with the realisability of a state of matter beyond the hadronic one, for $\alpha \leq 7/2$, our results seem to open anew the issue whether this particular value for α is compatible with the existence of a new phase beyond the Hagedorn temperature. Secondly, according to Letessier and Tounsi [14] the anomaly of the Bootstrap model, signifying the termination of the hadronic world, persists in the thermodynamic limit and is, therefore, genuinely connected with a phase transition only for $\alpha > 5/2$. Once again, the $\alpha = 2$ version of the SBM fails to meet the desired criterion.

It is clear that all the above objections, whether on the phenomenological or the purely theoretical front, are automatically removed for the $\alpha = 4$ version of the SBM. Moreover, for

³Indeed, as we have seen, it made no difference whether our description was based on strangeness, or strangeness density. Equivalently, the bag constant B which enters finite volume corrections did not figure into our final results.

this case we have the strong consequence that T_0 , the critical temperature for zero chemical potentials, is in a one- to-one correspondence with the bag constant B . Here we have the intriguing possibility of cross checking QCD lattice input, which aims at the determination of T_0 on the one hand and phenomenological information related to the bag constant B on the other. In Table 2 we exhibit the connection between T_0 and B values, as provided by the $\alpha = 4$ SBM⁴.

To summarise, the $\alpha = 4$ case represents, in all respects, a self consistent model which seems best suited to approach the problem of (possible) QGP formation in relativistic, heavy nucleus-nucleus collisions from the hadronic side. On this basis we shall take up in the next Section numerical determinations of strange particle production ratios which are directly relevant to experimental observation.

| T_0 (MeV) | $B^{1/4}$ (MeV) |
|-------------|-----------------|
| 150 | 155.494 |
| 160 | 178.128 |
| 170 | 202.419 |
| 180 | 228.231 |
| 190 | 255.424 |
| 200 | 283.859 |

Table 2. Connection between T_0 and B .

6. Study of (strange) Particle Ratios through $\alpha=4$ SBM version

Particle ratios for given pairs of hadronic species, strange in particular, emerging from a heavy nucleus-nucleus collision region, constitutes an accessible experimental measurement for which a data base is readily available [18]. In the framework of our thermal description

⁴From this point on, numerical assignments to physical quantities such as T_0 , B etc. employ updated results [18] with respect to what was used in [9].

of the multi-particle system generated via the aforementioned type of collisions such particle ratios can be computed, as functions of T , μ_q and μ_s , from our partition function. A pioneering work, in this connection and within framework of what we have been referring to as the “ideal hadron gas model”, has been performed by Cleymans and Satz [19]. Recall that the ideal hadron gas model furnishes a thermal description of the multi-hadron system without SBM input. In what follows we shall adjust the theoretical determination of particle ratios to SBM constraints. Clearly, their evaluation at the critical surface, for different values of T_0 , is directly pertinent to multi-particle production from the critical system.

Given our reasons, in favour of the $\alpha = 4$ version of the SBM, our considerations will be restricted to this case. A quintessential ingredient of our intended analysis is the inclusion of fugacities corresponding to **hadron species** [20] in terms of which particle ratios should be given. Their introduction into our formalism enters at the level of equations (10), (11) and (16) for the φ and G terms of the bootstrap equations and the partition functions, respectively. In this way, we produce generalisations of the form, e.g. in the partition function case,

$$Z(V, \beta, \lambda_q, \lambda_s) \rightarrow Z(V, \beta, \lambda_q, \lambda_s, \dots, \lambda_i, \dots) , \quad (55)$$

where λ_i represents the fugacity of the i th hadron.

In our thermal description the total number of the particle i is given by

$$N_i^{th} = \left(\lambda_i \frac{\partial \ln Z(V, \beta, \lambda_q, \lambda_s, \dots, \lambda_i, \dots)}{\partial \lambda_i} \right) \Big|_{\dots=\lambda_i=\dots=1} , \quad (56)$$

where “*th*” stands for thermal.

Referring to (42) we write, for the $\alpha = 4$ version of the SBM,

$$N_i^{th}(V, T, \lambda_q, \lambda_s) = \frac{VT^3}{4\pi^3 H_0} \int_0^T \frac{1}{y^5} \frac{1}{2 - \exp[G(y, \lambda_q, \lambda_s)]} \frac{\partial \varphi(y, \lambda_q, \lambda_s, \dots, \lambda_i, \dots)}{\partial \lambda_i} \Big|_{\dots=\lambda_i=\dots=1} dy. \quad (57)$$

Our approach to the data should also take into account the fact that experiments measure, as a rule, the products of resonance decays. Accordingly, we shall refer to the number of particles which also includes secondary production processes. We thereby deal with particle numbers N_i which, for a given species, have the form

$$N_i(V, T, \lambda_q, \lambda_s) = N_i^{th}(V, T, \lambda_q, \lambda_s) + \sum_j b_{ij} N_j^{th}(V, T, \lambda_q, \lambda_s) , \quad (58)$$

where the b_{ij} are branching ratios corresponding to the decay of resonance j into the observed hadron species labelled by i .

Switching to particle densities, since as the volume drops out in the ratio the volume corrections become irrelevant, equations (57) and (58) determine quantities of the form ($i \neq j$)

$$\frac{n_i}{n_j}(T, \lambda_q, \lambda_s) \equiv X_{ij}(T, \lambda_q, \lambda_s) . \quad (59)$$

Imposition of the condition $\langle S \rangle \geq 0$ yields equation (45), which furnishes a constraint among the thermodynamical variables T , λ_q and λ_s and enables us to eliminate one of them in (59).

In figures 12a-12i we depict various ratios involving at least one strange particle, for the $\alpha = 4$ version of the SBM, as functions of the temperature T for constant fugacity λ_q (μ_q/T fixed at 0.4 in these examples) and for different values of T_0 . In each case we present the curve stemming from the ideal hadron gas model, for comparison purposes.

We next turn our attention to critical values of particle ratios, namely ratios evaluated on the intersection between the critical and the $\langle S \rangle \geq 0$ surfaces. Our study will be conducted on the basis of adopting the critical temperature T_{cr} as our independent variable. The results of our numerical analyses for different values of T_0 are depicted in figures 13a-13i.

The issue of greatest interest is an assessment of how close, according to our theoretical description, are current experimental data to the border of the hadronic world. To this end, let us remove the criticality constraint and test the proximity of actual data to it. Fixing the theoretical quantity (59) to its experimental value x_{ij}^{exp} , as recorded in observations from nucleus-nucleus collisions, we set

$$\frac{n_i}{n_j}(T, \lambda_q, \lambda_s) = x_{ij}^{exp} \pm \delta x_{ij}^{exp} , \quad (60)$$

where δx_{ij}^{exp} is the experimental error in the measurement of the quantity x_{ij}^{exp} . With the use of (45) we can eliminate one of the three thermodynamical quantities, e.g. λ_s , and arrive at two equations of the form

$$\frac{n_i}{n_j}(T, \lambda_q) = x_{ij}^{exp} - \delta x_{ij}^{exp} \quad , \quad \frac{n_i}{n_j}(T, \lambda_q) = x_{ij}^{exp} + \delta x_{ij}^{exp} . \quad (61)$$

The above equations define a band of values in the (T, μ_q) plane which are compatible with (60). Consider now a second particle ratio, say $\frac{n_k}{n_l}$ ($k \neq l$, $k \neq i$ and/or $j \neq l$).

Repeating the same procedure we determine a second band in the (T, μ_q) plane. If the region of intersection of two bands has a part **inside** the region bounded by the critical surface (Fig. 14a) then, according to our theoretical proposal, the experimentally recorded ratios are compatible with multiparticle production within the hadronic phase. If, on the other hand, the intersection of the two bands occurs completely **outside** the critical surface (Fig. 14b), then the situation merits further consideration. Indeed, one could consider the possibility that emission has occurred from an equilibrated QGP state before the latter has reached the critical point and subsequently the content of the system as a whole transformed into hadrons which equilibrated and immediately afterwards freed-out. Clearly, all this is based on our assumption of thermal and chemical equilibrium. A departure from equilibrium conditions may alter this conjecture.

When confronting specific experimental data it is important to eliminate every possibility that recorded particle ratios could come from a genuine hadronic phase. To this end we must consider the largest possible value of the MIT bag constant B , which maximises the value of T_0 and, consequently, of the space occupied by the hadronic domain. From [21,22] we are informed that

$$B^{1/4} = (145 - 235) \text{ MeV} . \quad (62)$$

The above range of values of B corresponds to a maximum critical temperature in the range of

$$T_0 \approx (145 - 183) \text{ MeV} . \quad (63)$$

To exhaust all available space for the hadronic phase we adopt the upper value of T_0 , i.e. $T_0 \approx 183 \text{ MeV}$. It is of interest to note that this particular value of T_0 leads to $\mu_{s \text{ cr}}$ at the end of the hadronic phase (for the case $\alpha = 4$) with values closest to zero, but without becoming negative (see Fig. 10a). A relevant study pertaining to data on particle ratios from the experiments at AGS (Brookhaven) and SPS (CERN), within the theoretical bounds set by this value of T_0 , is currently in progress [23].

7. Concluding Remarks

Our basic effort, in this paper, was to enlarge the SBM scheme so as to incorporate the strangeness quantum number. Such an attempt is *a priori* justified in view of the association of strangeness with one of the key experimental signals for the QGP state of matter, expected to be achieved in ultrarelativistic nucleus-nucleus collisions. Our efforts were directed towards the determination, in the 3-dimensional (T, μ_q, μ_s) space, of : 1) the critical surface, determined by the bootstrap equation, which sets the limits of the hadronic phase and 2) the $\langle S \rangle = 0$ surface, relevant to hadronic processes, which is determined from the partition function.

We restricted our attention to two different versions of the extended SBM, corresponding to the values $\alpha = 2$ and $\alpha = 4$ of the exponent which enters the asymptotic expression for the mass spectrum $\rho(m)$, cf. equ. (23). The first has dominated SBM studies in the past, in the absence of the strangeness quantum number. The numerical studies performed in this paper revealed decisive, physically motivated, advantages of the $\alpha = 4$ version of the strangeness-containing SBM. In addition, one now has the phenomenological advantage of uniquely relating the MIT bag constant to the critical temperature T_0 .

Finally, we considered the issue of produced particle ratios for cases where at least one of the two species carries strangeness. The relevant study has been conducted within the $\alpha = 4$ version of the SBM. Taking into account the constraint furnished by $\langle S \rangle = 0$, we have presented numerical results pertaining to particle ratios along a fixed direction in the (T, μ_q) plane which show: (a) for points well inside the hadronic domain the ratios coincide with those of the “ideal hadron gas model”, (b) as the critical surface is approached (bootstrap input) departure from the ideal description begin to show up. We also presented results on critical particle ratios, as a function of the (critical) temperature, along the intersection curve of the $\langle S \rangle = 0$ and critical surfaces.

Clearly, the present effort constitutes only a first step towards an increasingly complete investigation of multi-hadron production systems, coming from heavy-ion collisions, under the assumption of thermalization on the hadronic side. Obvious theoretical refinements are: (1) The differentiation between the up-down quantum numbers (isospin breaking effects) which will introduce separate chemical potentials μ_u , μ_d in place of μ_q . On the hadronic

side this entails the extension $\lambda_B \rightarrow (\lambda_B, \lambda_Q)$, where λ_Q is the fugacity corresponding to total charge and (2) The introduction into our description of the variable $\gamma_s^2 = \lambda_s^{neq} \lambda_{\bar{s}}^{neq} \neq 1$, where “*neq*” stand for “non-equilibrium”, pertaining to a measure of *partial* strangeness equilibrium.

On a broader basis, of course, lies the problem of how to relate information obtained from the hadronic side on the one hand, with QCD-related input coming from the QGP phase of matter on the other. The outlook for investigations of this nature clearly has a longer range prospective.

As already mentioned, work is now in progress which addresses itself to actual experimental data on (strange) particle ratios. The aim of such an effort is to identify, always according to the $\alpha = 4$ version of the extended SBM, whether the multiparticle source, which furnishes a particular set of data, lies inside or outside the bounds of the phase of hadrons. In a forthcoming paper [23] we shall present the results of such analyses.

Acknowledgements

We wish to thank Prof. R. Hagedorn for useful discussions. A. S. K. also wishes to thank Dr. C. G. Papadopoulos for discussion and guidance in certain parts of the numerical calculations.

This work was partially supported by the programme ΠΕΝΕΔ No. 1361.1674/31-1-95, Gen. Secretariat for Research and Technology, Hellas.

References

- [1] R. Hagedorn, Suppl. Nuovo Cimento **3**, 147 (1965); R. Hagedorn and J. Ranft, Suppl. Nuovo Cimento **6**, 311 (1968); *ibid* **6**, 311 (1968)
- [2] R. Hagedorn, 1985 “Springer Lecture Notes in Physics”, **221** ed. K. Kajantie (Berlin, Heidelberg, New York) p.53
- [3] R. Hagedorn, 1995 “Hot Hadronic Matter” NATO-ASI-Series **B346** eds. J. Letessier et. al., p.13
- [4] S. Frautschi, Phys. Rev. **D3**, 2821 (1971)
- [5] B. Touschek, Nuovo Cimento **28B**, 295 (1968)
- [6] N. Cabibbo and G. Parisi, Phys. Lett. **59B**, 67 (1975)
- [7] L. D. McLerran and B. Svetitsky, Phys. Lett. **98B**, 195 (1981); J. Kuti, J. Polonyi and K. Szlachanyi, Phys. Lett. **98B**, 199 (1981); J. Engels, F. Karsch, I. Montvay and H. Satz, Nucl. Phys. **B205** [FS5], 545 (1982); *ibid* Phys. Lett. **101B**, 89 (1981)
- [8] C. J. Hamer and S. C. Frautschi, Phys. Rev. **D4**, 2125 (1971)
- [9] A. Chodos, R. L. Jaffe, K. Johnson, C. B. Thorn, V. F. Weisskopf, Phys. Rev. **D9**, 3471 (1974)
- [10] A. S. Kapoyannis, C. N. Ktorides and A. D. Panagiotou, J. Phys. G23, 1921, (1997)
- [11] R. Hagedorn, I. Montvay and J. Rafelski, “*Hadronic Matter at Extreme Energy Density*”, eds. N. Cabibbo and L. Sertorio, Plenum Press, New York, 49 (1980)
- [12] R. Fiore, R. Hagedorn and F. d’ Isep, Nuovo Cimento **88A**, 301 (1985)
- [13] W. Nahm, Nucl. Phys. **B45**, 525 (1972); R. Hagedorn and I. Montvay, Nucl. Phys. **B59**, 45 (1973)
- [14] J. Letessier and A. Tounsi, Nuovo Cimento **99A**, 521 (1988)

- [15] R. Hagedorn and J. Rafelski, Phys. Lett. **97B**, 136 (1980)
- [16] J. Cleymans, K. Redlich, H. Satz, E. Suhonen, Z. Phys. **C58**, 347 (1993)
- [17] M. N. Asprouli and A. D. Panagiotou, Phys. Rev. **D51** 1086 (1995); A. D. Panagiotou, G. Mavromanolakis and J. Tzoulis, Phys. Rev. **C53** 1353 (1996)
- [18] R. M. Barnett et. all, (Particle Data Group), Phys. Rev. **D54** (1996)
- [19] J. Cleymans and H. Satz, Z. Phys. **C57**, 135 (1993)
- [20] R. Hagedorn and K. Redlich, CERN preprint, TH.3889, (1984)
- [21] W. C. Haxton and L. Heller, Phys. Rev. **D22**, 1198 (1980)
- [22] P. Hasenfratz, R. R. Horgan, J. Kuti and J. M. Richard, Phys. Lett. **95B**, 199 (1981)
- [23] A. S. Kapoyannis, C. N. Ktorides and A. D. Panagiotou, paper in preparation.

Figure Captions

Figure 1 G as a function of φ . The branch point sets a limit on the hadronic description of matter.

Figure 2 (a) Intersections of planes of constant s-quark chemical potential μ_s with the critical surface $\varphi(T, \mu_q, \mu_s) = \ln 4 - 1$ for $\alpha = 2$ and for $T_0 = 180$ MeV. (b) Intersections of planes of constant q-quark chemical potential μ_q with the critical surface $\varphi(T, \mu_q, \mu_s) = \ln 4 - 1$ for $\alpha = 2$ and for $T_0 = 180$ MeV.

Figure 3 (a) Variation of the intersection of the plane of constant s-quark chemical potential $\mu_s = 0$ with the critical surface $\varphi(T, \mu_q, \mu_s) = \ln 4 - 1$, for $\alpha = 2$, for different values of T_0 . (b) Variation of the intersection of the plane of constant q-quark chemical potential $\mu_q = 0$ with the critical surface $\varphi(T, \mu_q, \mu_s) = \ln 4 - 1$, for $\alpha = 2$, for different values of T_0 .

Figure 4 Projection on the plane (T, μ_s) of intersections of planes of constant q-quark fugacity λ_q ($\mu_q/T = 0.4$) with the surface $\langle S \rangle \geq 0$ for different values of T_0 , for the $\alpha = 2$ version of the SBM.

Figure 5 (a) Projection on the plane (μ_q, μ_s) of the intersection of the critical surface and the surface $\langle S \rangle \geq 0$ for the value of $\alpha = 2$. (b) Projection on the plane (T, μ_s) of the intersection of the critical surface and the surface $\langle S \rangle \geq 0$ for the $\alpha = 2$ version of the SBM.

Figure 6 (a) Intersections of planes of constant s-quark chemical potential μ_s with the critical surface $\varphi(T, \mu_q, \mu_s) = \ln 4 - 1$ for $\alpha = 4$ and for $T_0 = 180$ MeV. (b) Intersections of planes of constant q-quark chemical potential μ_q with the critical surface $\varphi(T, \mu_q, \mu_s) = \ln 4 - 1$ for $\alpha = 4$ and for $T_0 = 180$ MeV.

Figure 7 (a) Variation of the intersection of the plane of constant s-quark chemical potential $\mu_s = 0$ with the critical surface $\varphi(T, \mu_q, \mu_s) = \ln 4 - 1$ for $\alpha = 4$, for different values of T_0 . (b) Variation of the intersection of the plane of constant q-quark chemical potential $\mu_q = 0$ with the critical surface $\varphi(T, \mu_q, \mu_s) = \ln 4 - 1$, for $\alpha = 4$, for different values of T_0 .

Figure 8 (a) Comparison of the intersections of planes of constant s-quark chemical potential μ_s with the critical surface $\varphi(T, \mu_q, \mu_s) = \ln 4 - 1$ for the cases $\alpha = 2$ and $\alpha = 4$ and for $T_0 = 180$ MeV. (b) Comparison of the intersections of planes of constant q-quark chemical potential μ_q with the critical surface $\varphi(T, \mu_q, \mu_s) = \ln 4 - 1$ for the cases $\alpha = 2$ and $\alpha = 4$ and for $T_0 = 180$ MeV.

Figure 9 Projection on the plane (T, μ_s) of intersections of planes of constant q-quark fugacity λ_q ($\mu_q/T = 0.4$) with the surface $\langle S \rangle \geq 0$ for different values of T_0 , for $\alpha = 4$.

Figure 10 (a) Projection on the plane (μ_q, μ_s) of the intersection of the critical surface and the surface $\langle S \rangle \geq 0$ for $\alpha = 4$. (b) Projection on the plane (T, μ_s) of the intersection of the critical surface and the surface $\langle S \rangle \geq 0$ for $\alpha = 4$.

Figure 11 A three-dimensional perspective of our results for the $\alpha = 4$ version of the SBM. The set of rising and subsequently falling curves correspond to intersections of planes of constant λ_q with the surface $\langle S \rangle = 0$. The intersection of this surface with the critical one, for $T_0 = 183$ MeV, is the contour which lies on the edges of the former curves.

Figure 12 (a) The ratio K^+/π^+ as a function of temperature, for $\mu_q/T = 0.4$. (b) The ratio K^-/π^- as a function of temperature, for $\mu_q/T = 0.4$. (c) The ratio K^+/K^- as a function of temperature, for $\mu_q/T = 0.4$. (d) The ratio K_s^0/π^0 as a function of temperature, for $\mu_q/T = 0.4$. (e) The ratio $\Xi^+/\bar{\Lambda}$ as a function of temperature, for $\mu_q/T = 0.4$. (f) The ratio Ξ^-/Λ as a function of temperature, for $\mu_q/T = 0.4$. (g) The ratio $\bar{\Lambda}/\Lambda$ as a function of temperature, for $\mu_q/T = 0.4$. (h) The ratio K_s^0/Λ as a function of temperature, for $\mu_q/T = 0.4$. (i) The ratio $\bar{\Xi}^0/\Xi^0$ as a function of temperature, for $\mu_q/T = 0.4$. These ratios pertain to the $\alpha = 4$ version of the SBM.

Figure 13 (a) The critical value of the ratio K^+/π^+ as a function of the critical temperature. (b) The critical value of the ratio K^-/π^- as a function of the critical temperature. (c) The critical value of the ratio K^+/K^- as a function of the critical temperature. (d) The critical value of the ratio K_s^0/π^0 as a function of the critical temperature. (e) The critical value of the ratio $\Xi^+/\bar{\Lambda}$ as a function of the critical temperature. (f) The critical value of the ratio Ξ^-/Λ as a function of the critical temperature. (g) The critical value of the ratio $\bar{\Lambda}/\Lambda$ as a function of the critical temperature. (h) The critical value of the ratio K_s^0/Λ as a function of the critical temperature. (i) The critical value of the ratio $\bar{\Xi}^0/\Xi^0$ as a function of the critical temperature. These ratios pertain to the $\alpha = 4$ version of the SBM.

Figure 14 (a) A situation where two experimentally measured particle ratios can have hadronic origin. (b) A situation where two experimentally measured particle ratios would imply, under the assumption of thermalisation, that their origin is outside the domain of hadrons.

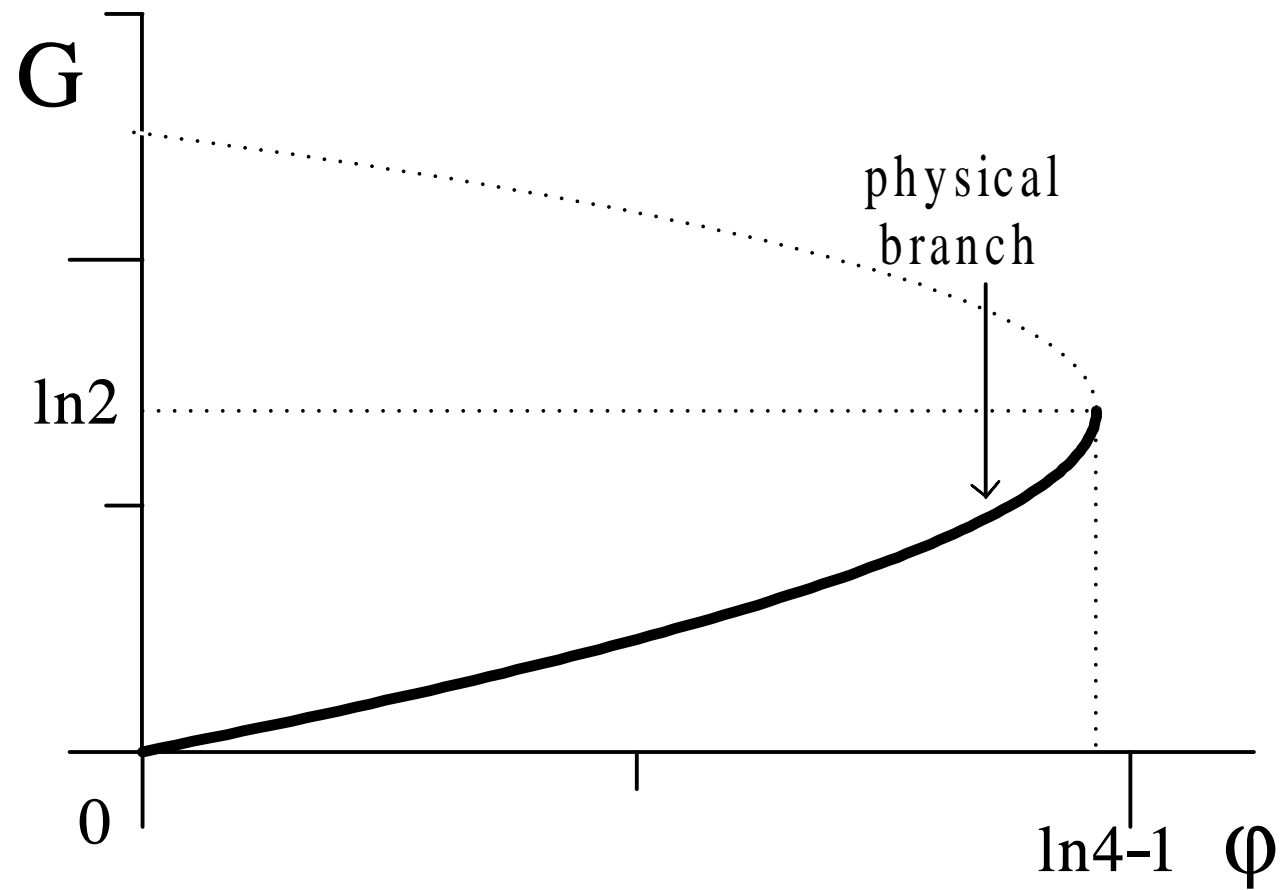


Fig. 1

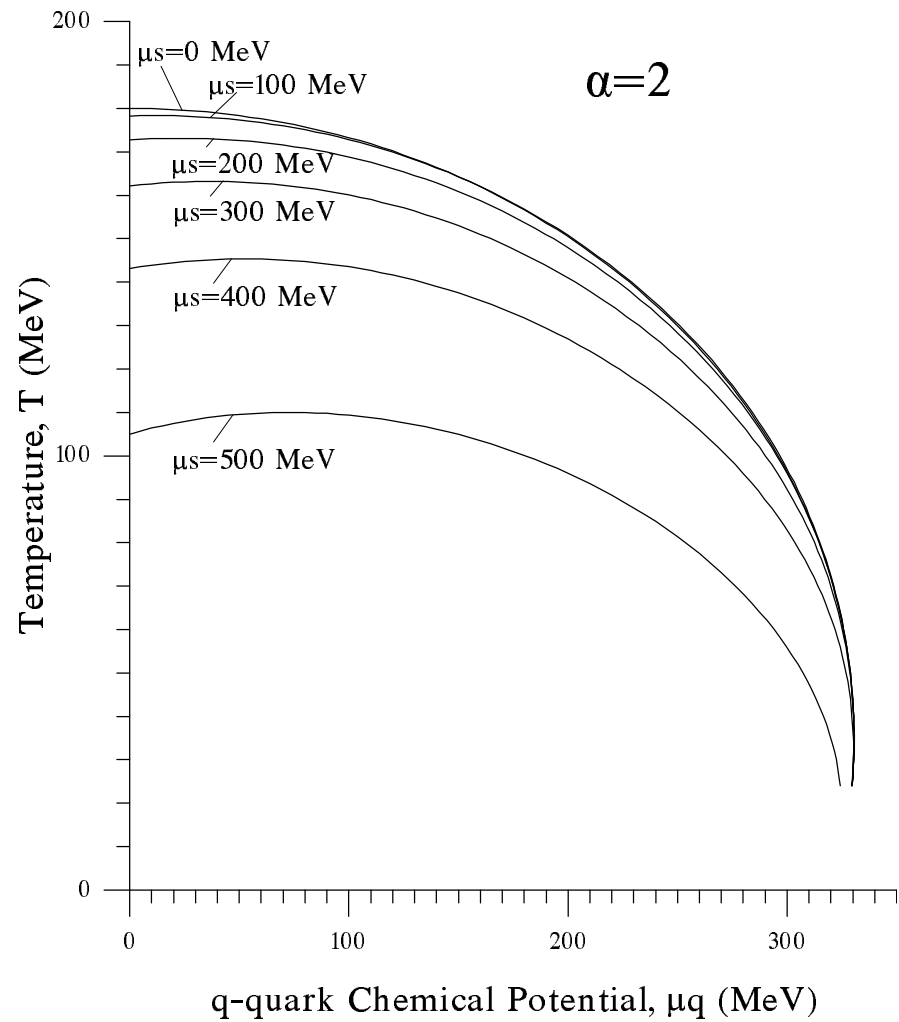


Fig. 2a

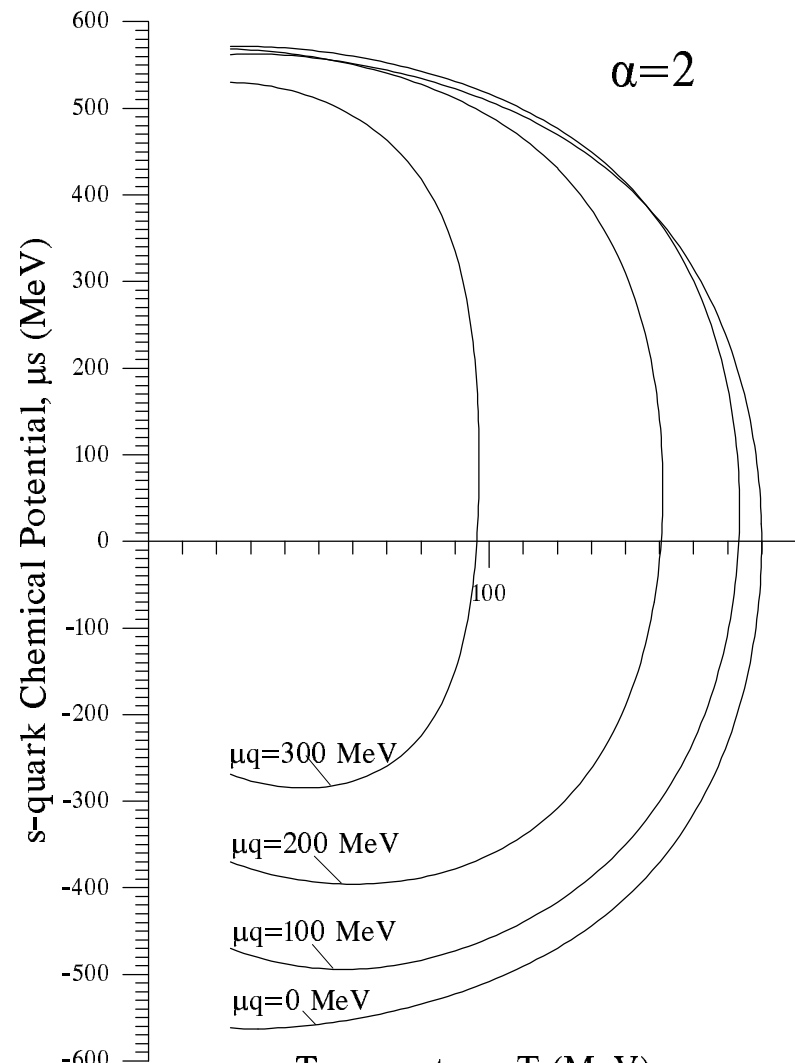


Fig. 2b

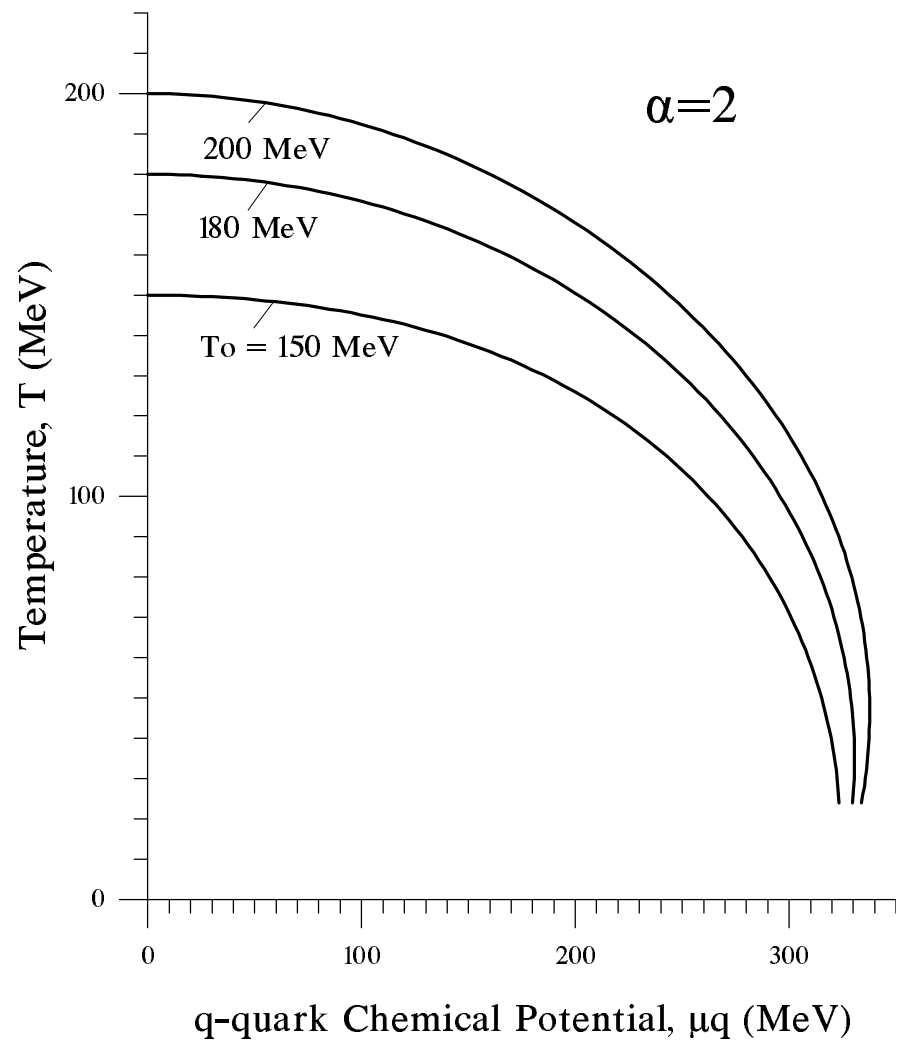


Fig. 3a

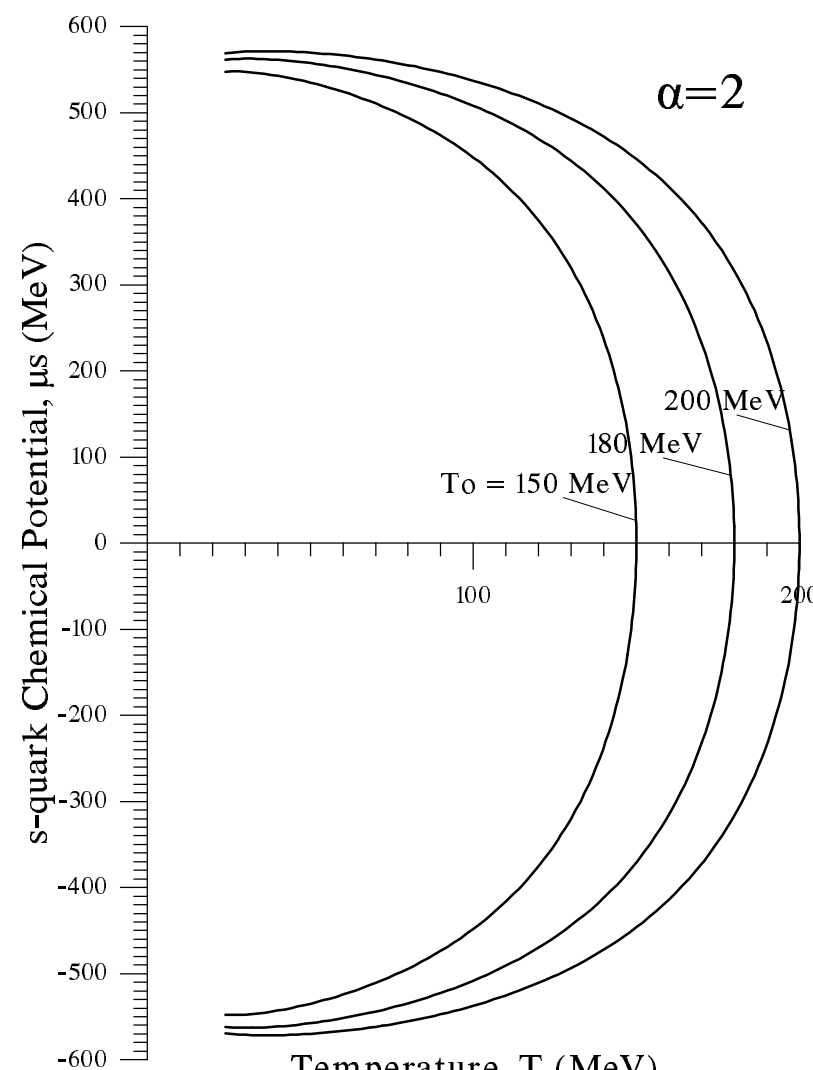


Fig. 3b

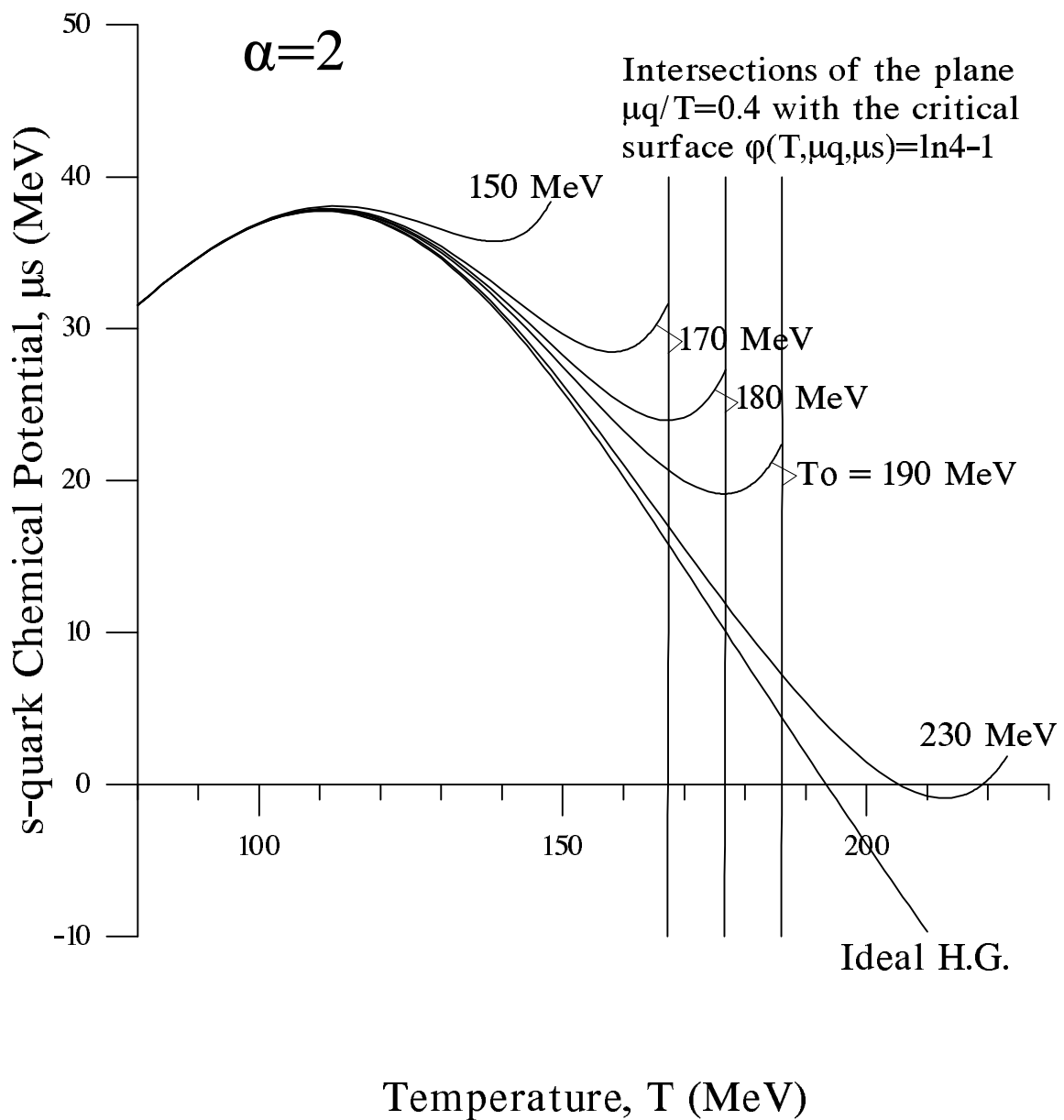


Fig. 4

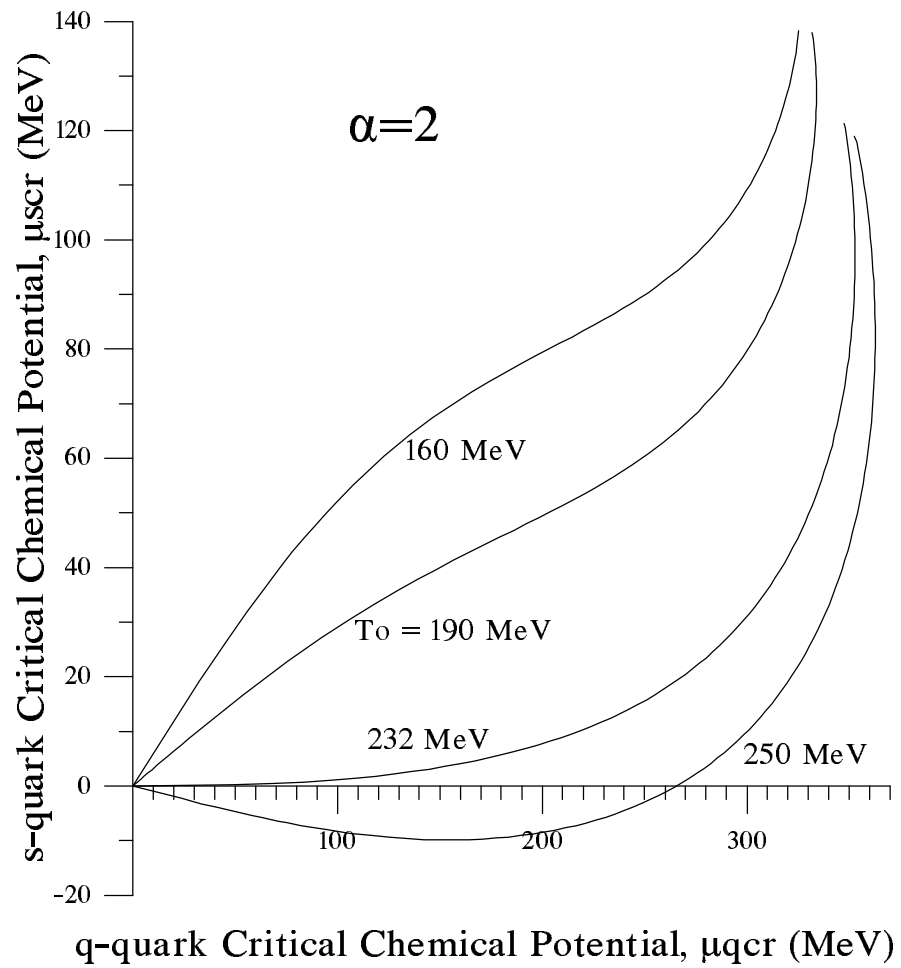


Fig. 5a

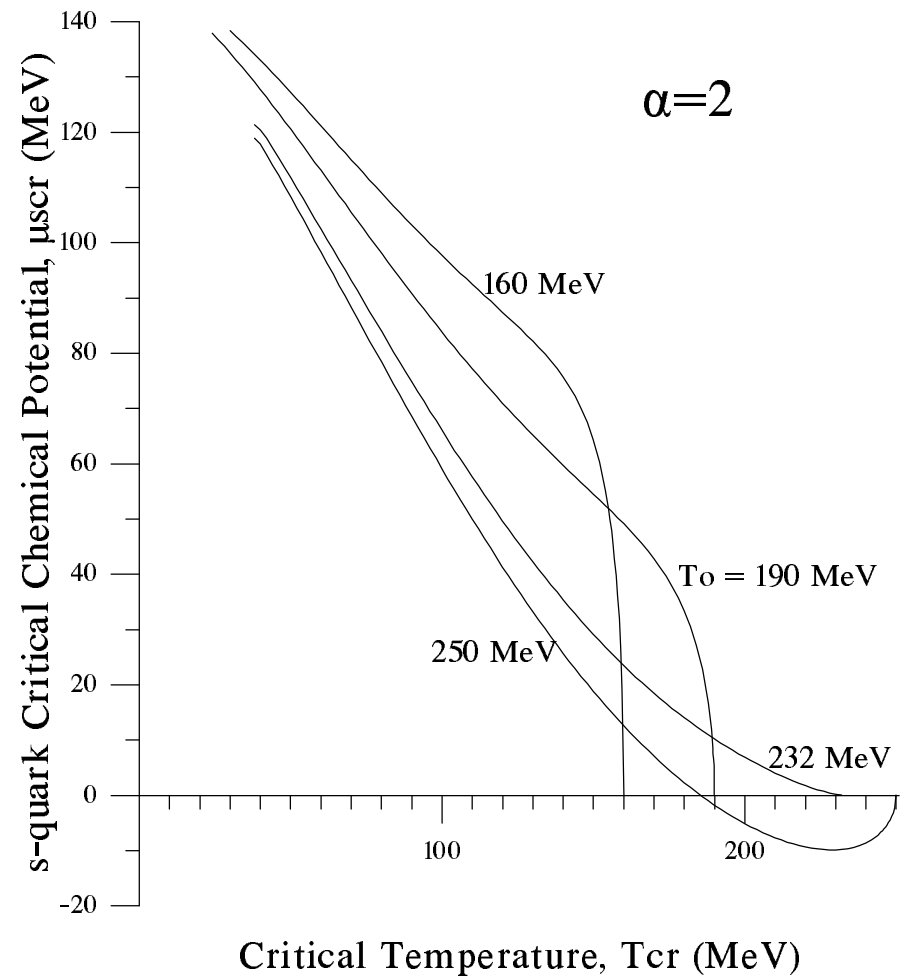


Fig. 5b

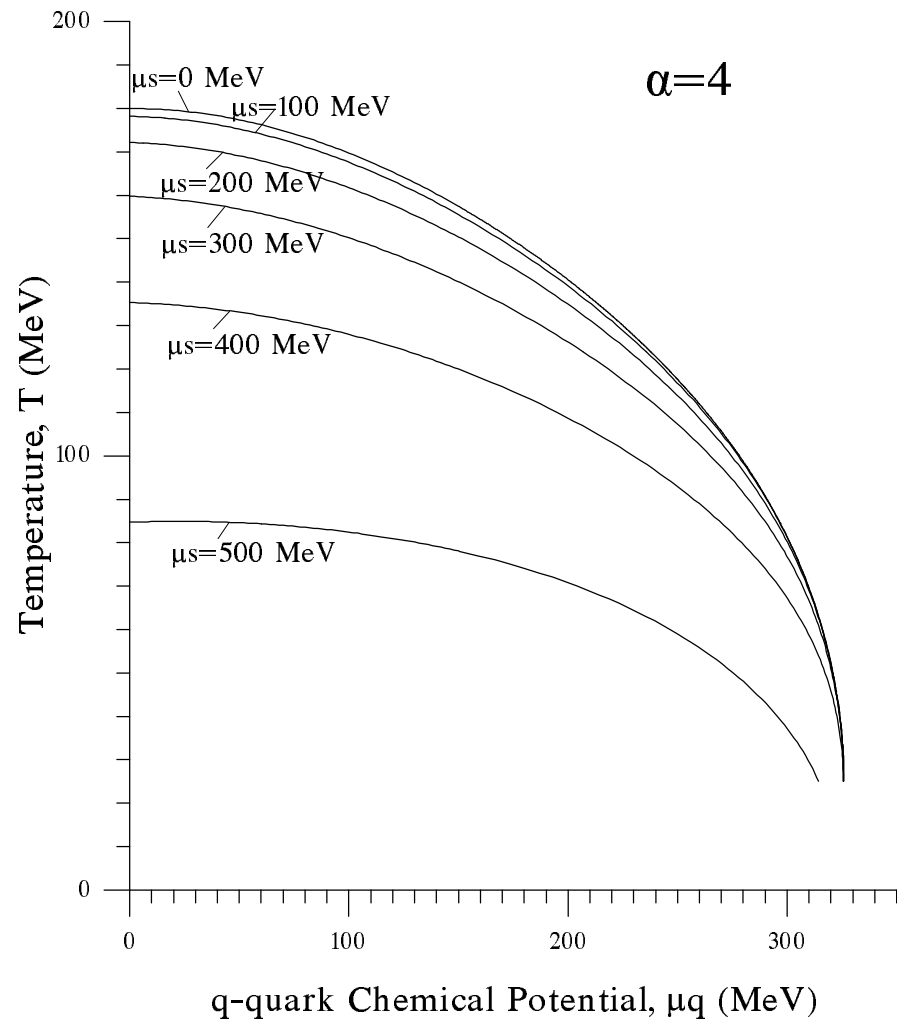


Fig. 6a

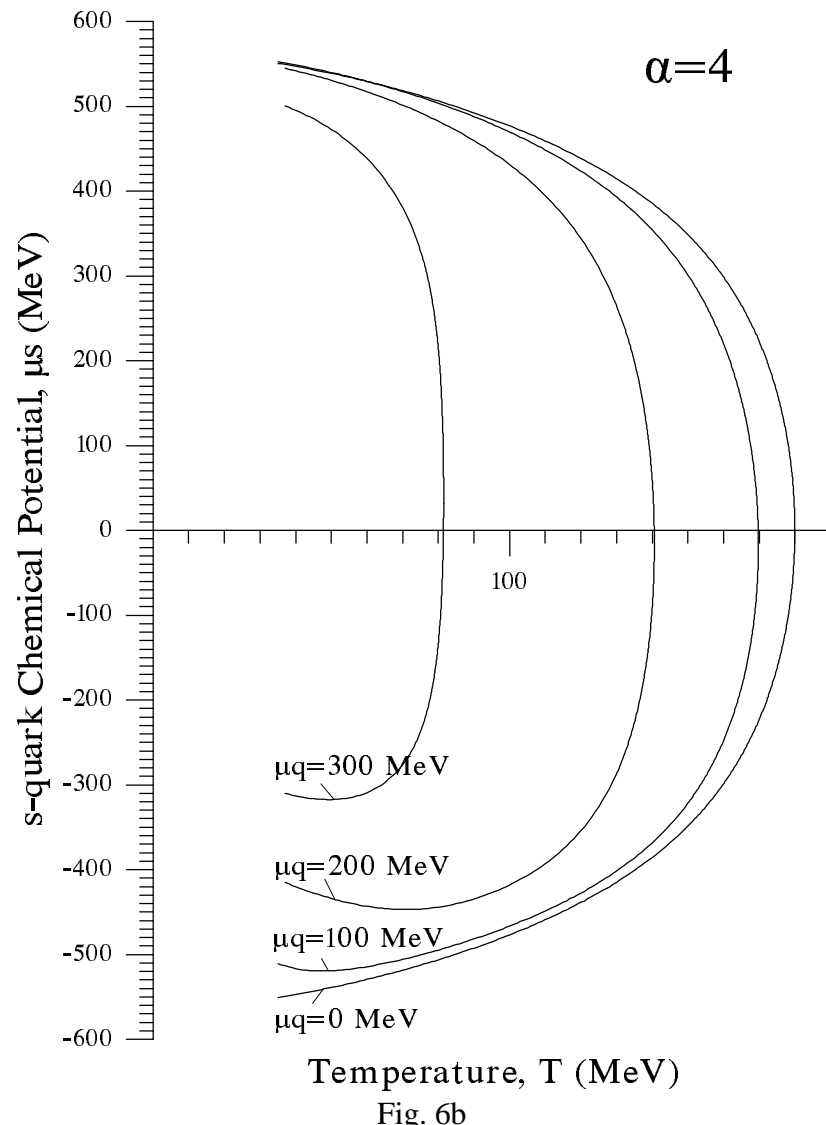


Fig. 6b

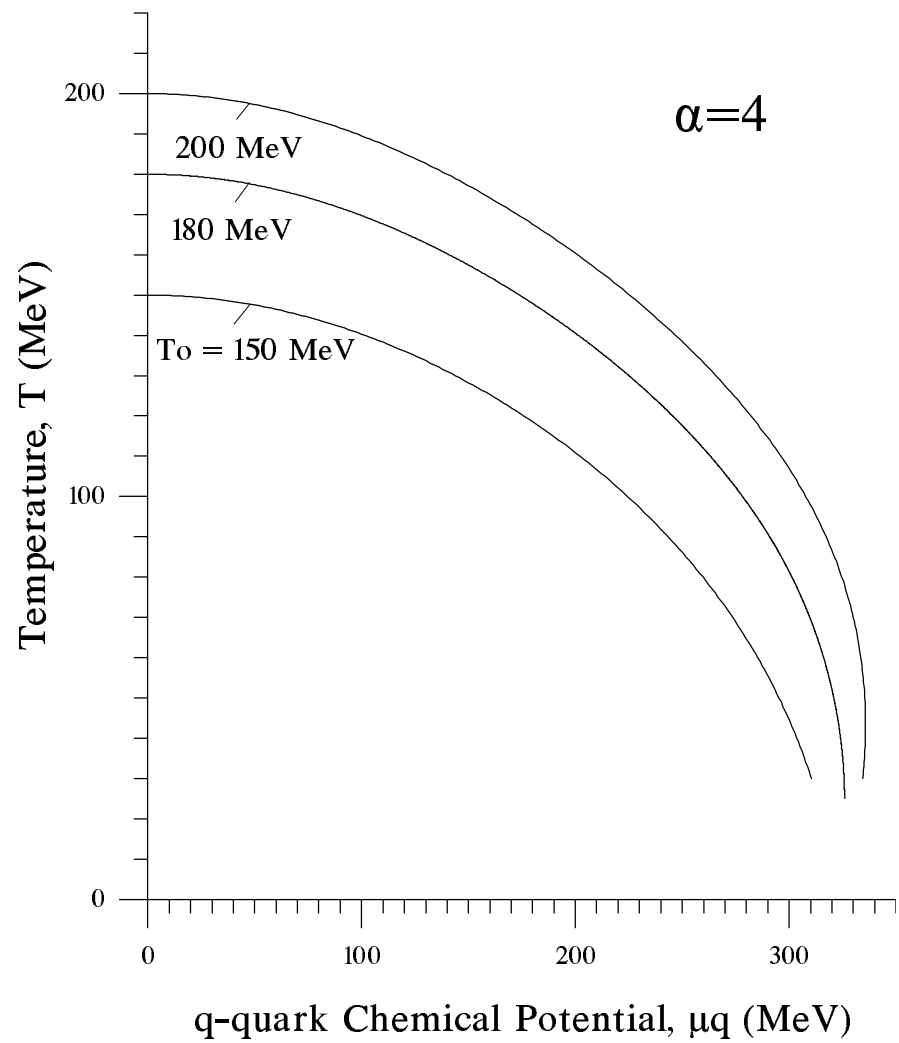


Fig. 7a

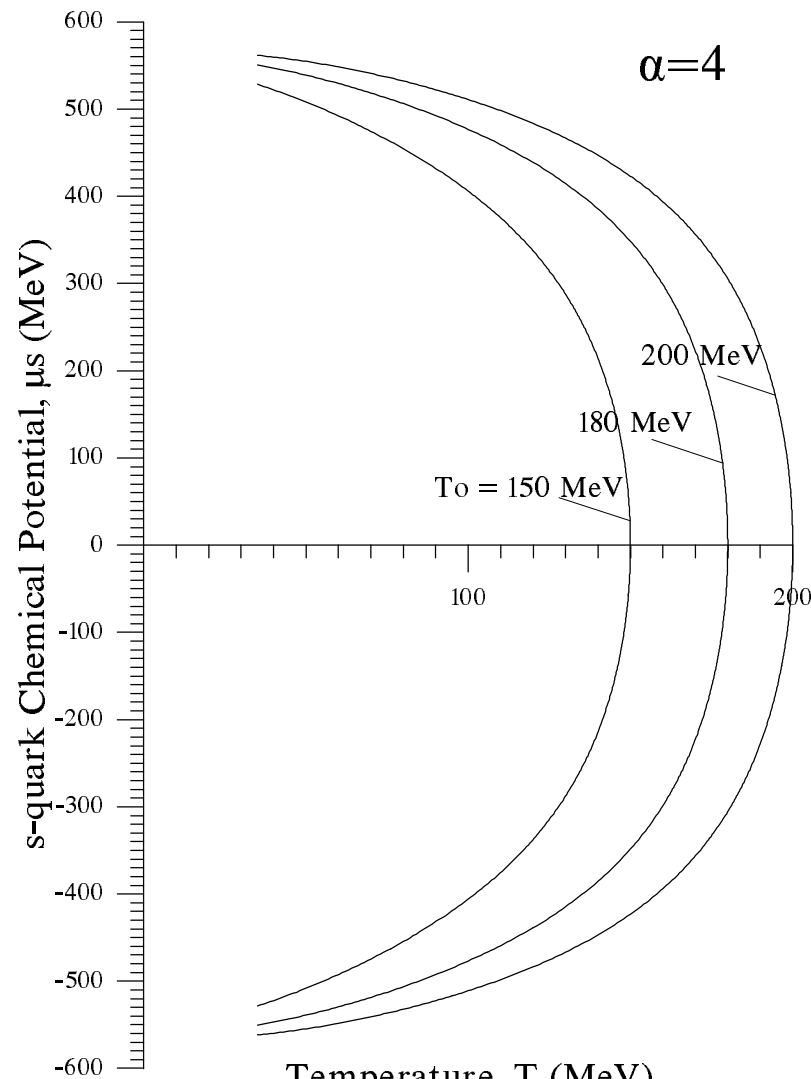


Fig. 7b

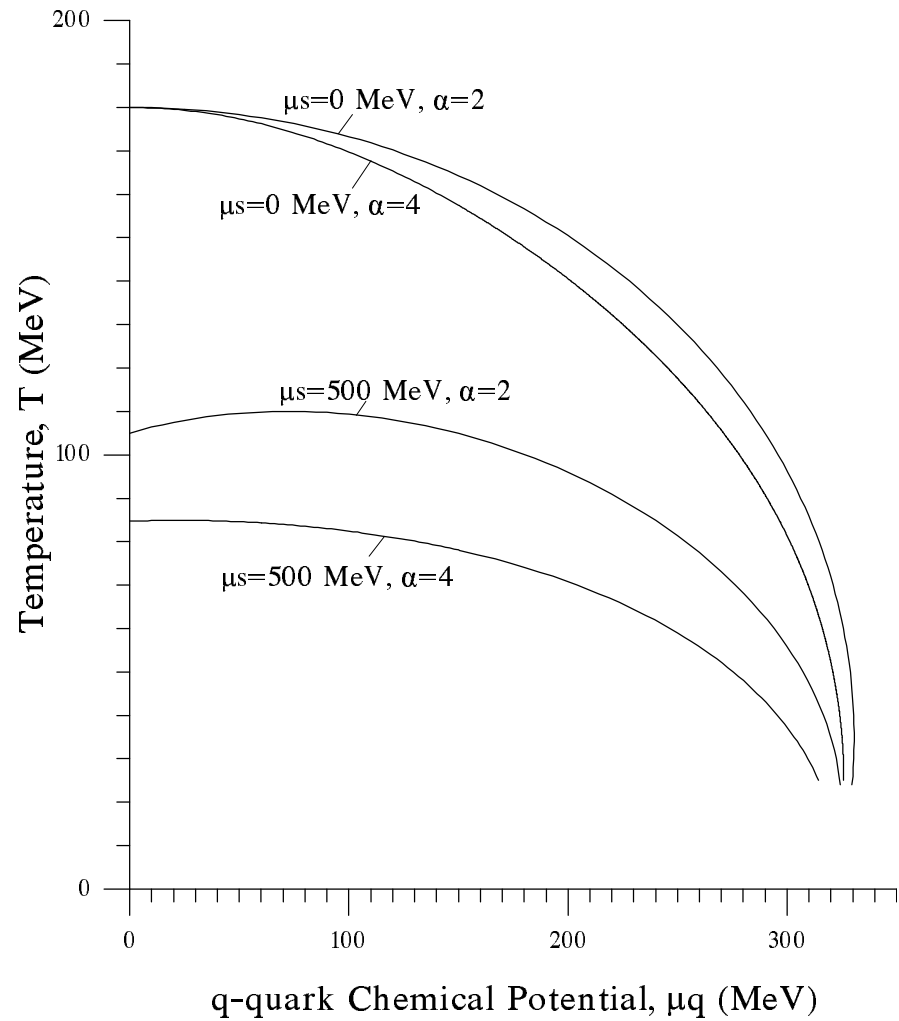


Fig. 8a

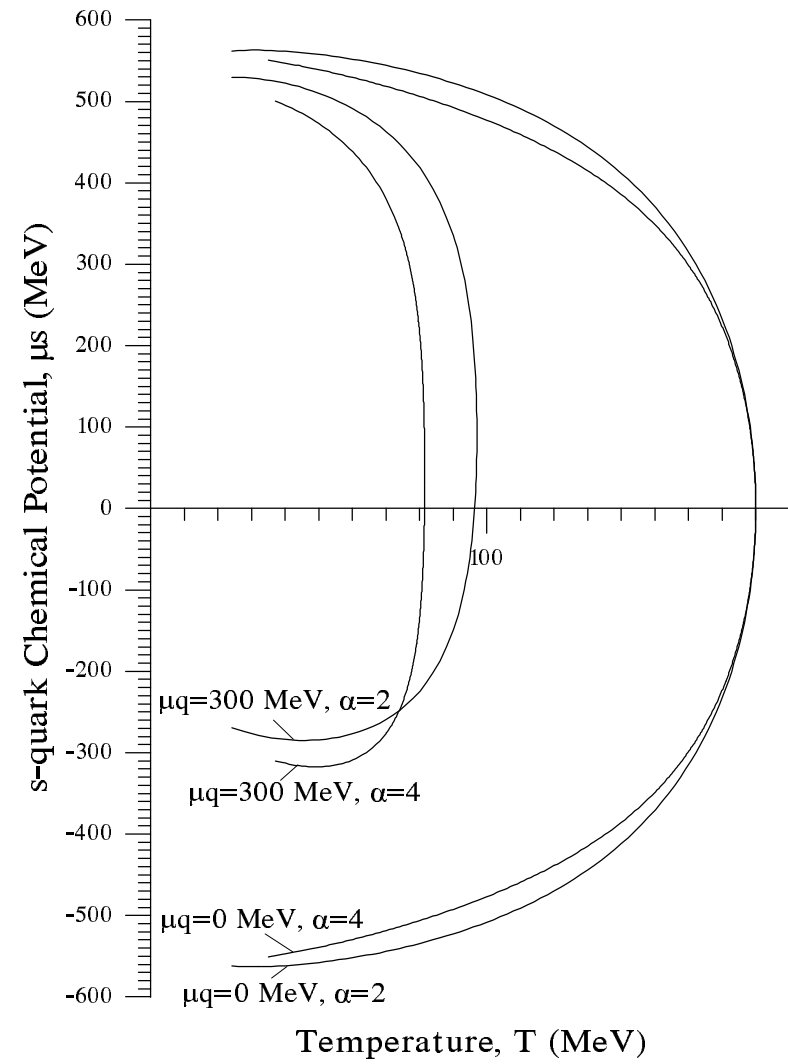


Fig. 8b

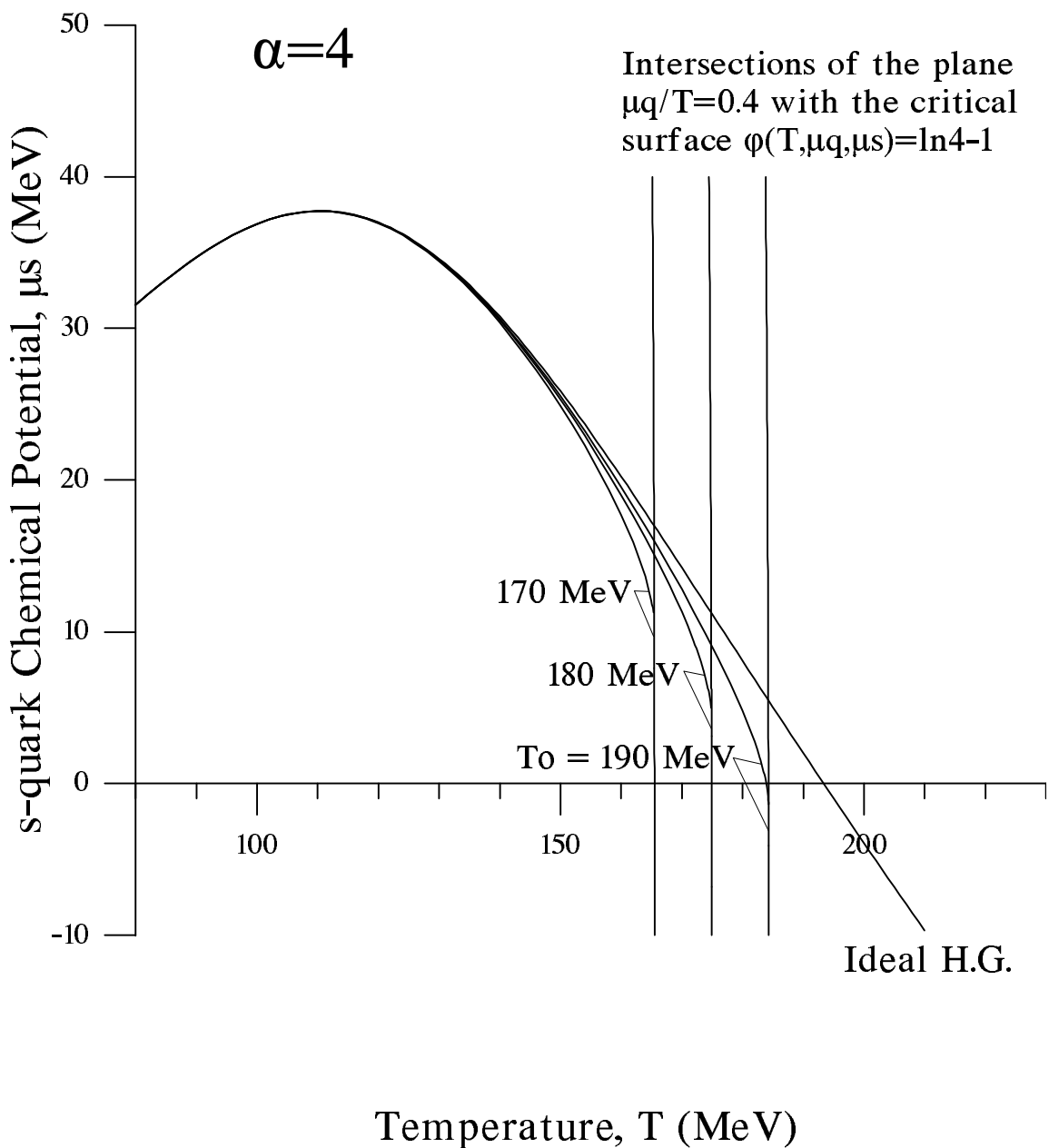


Fig. 9

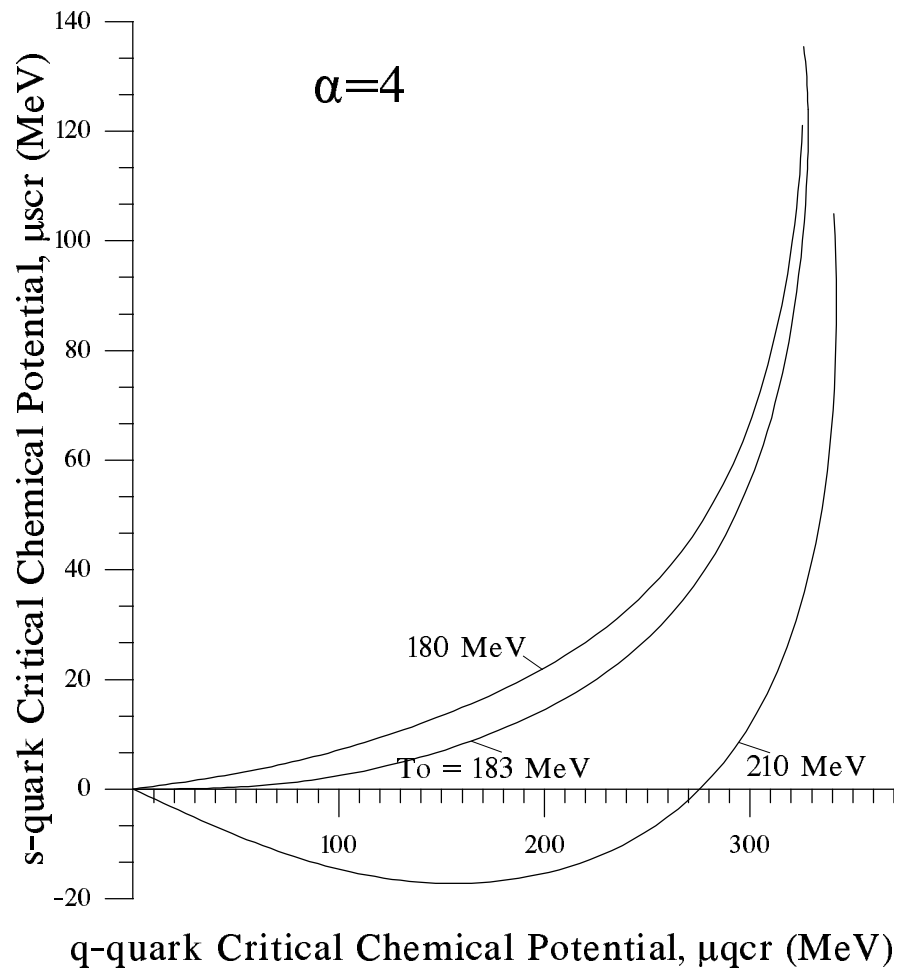


Fig. 10a

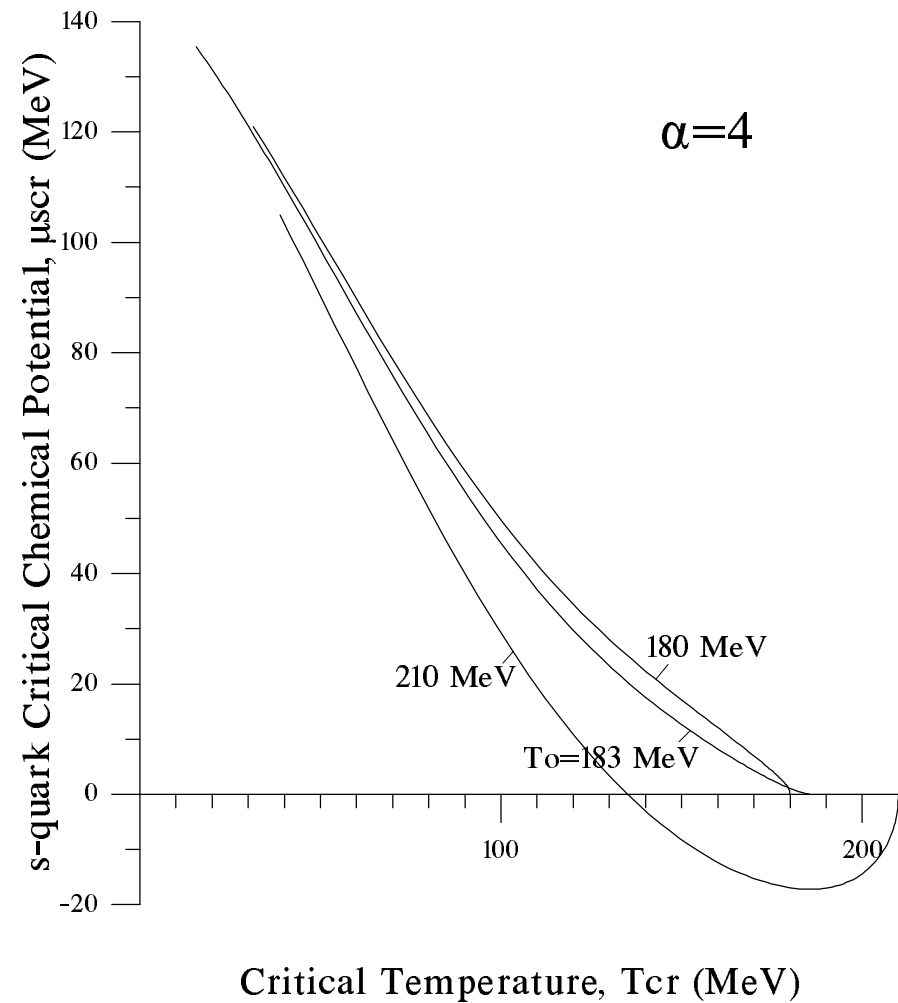


Fig. 10b

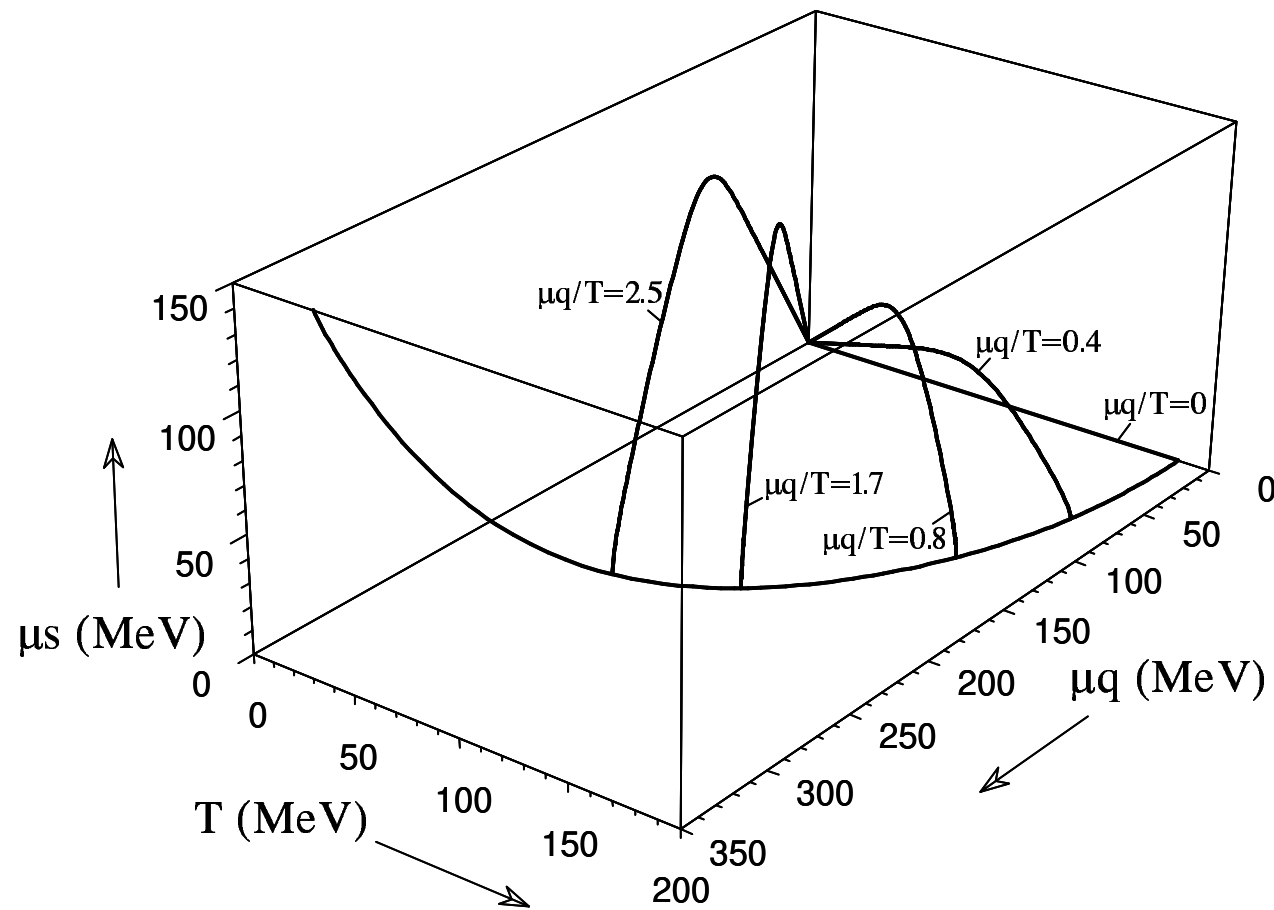


Fig. 11

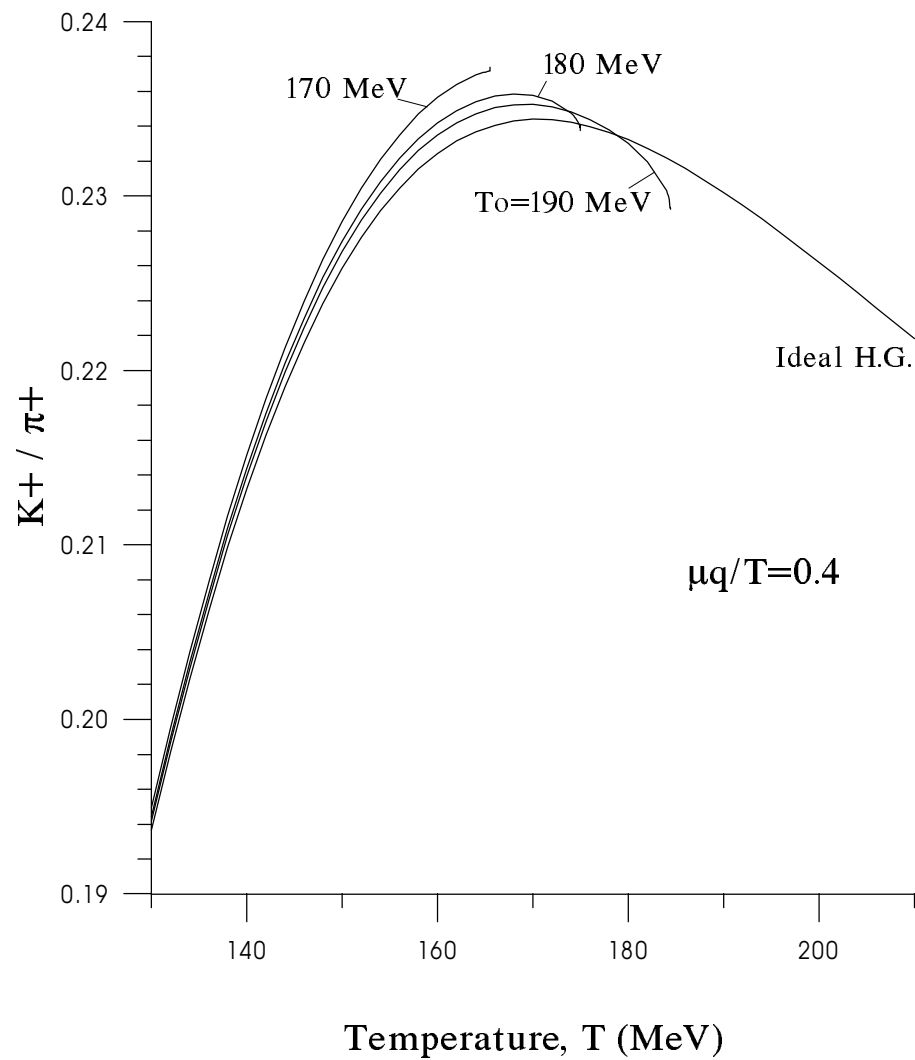


Fig. 12a

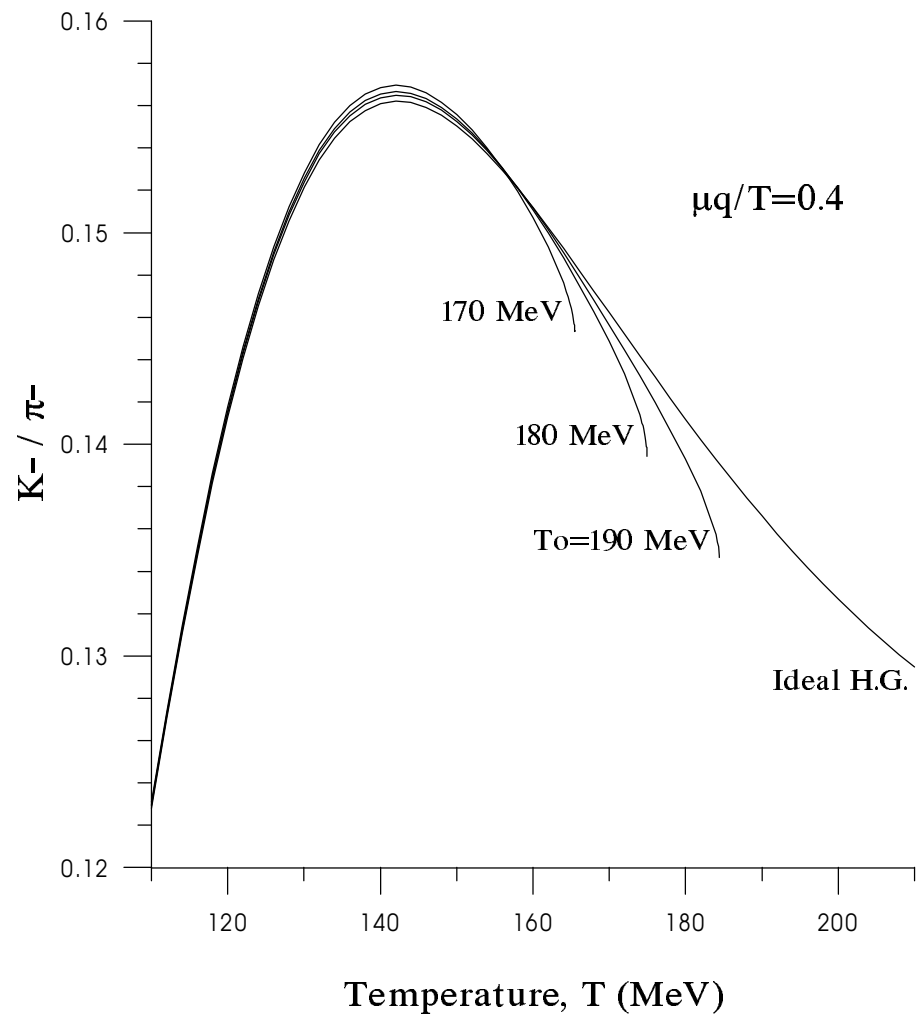


Fig. 12b

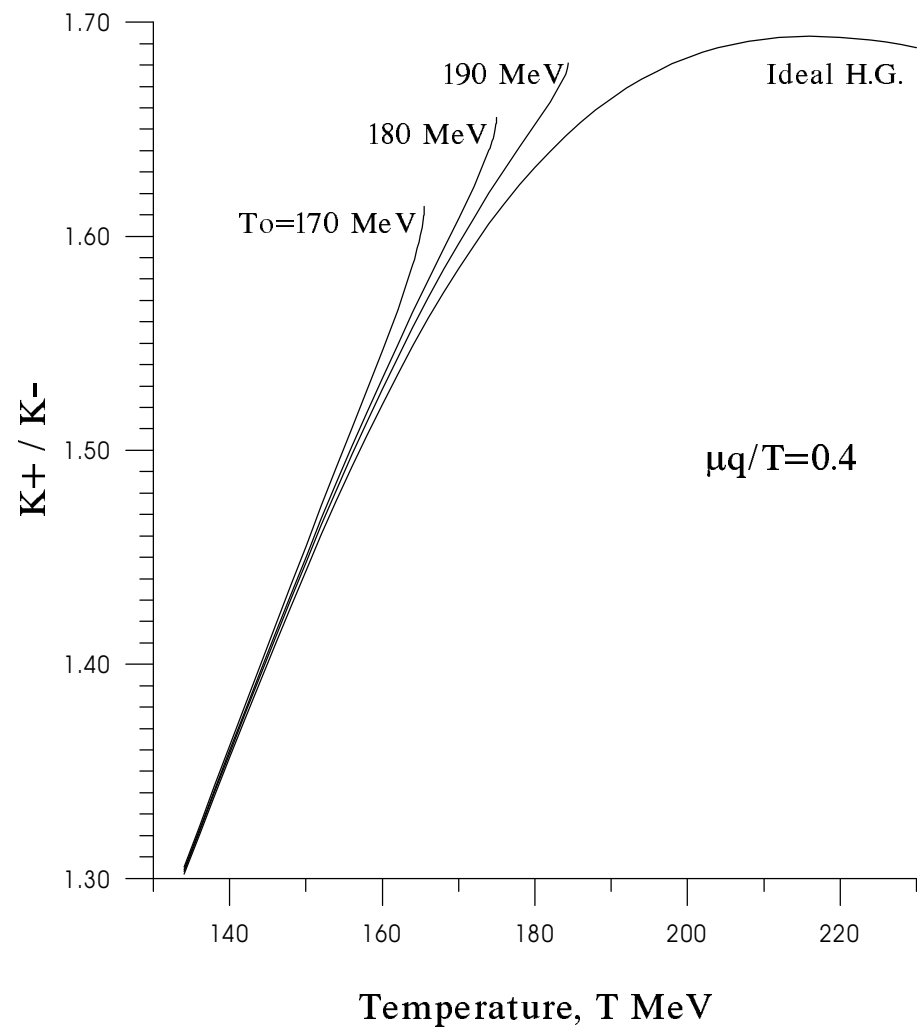


Fig. 12c

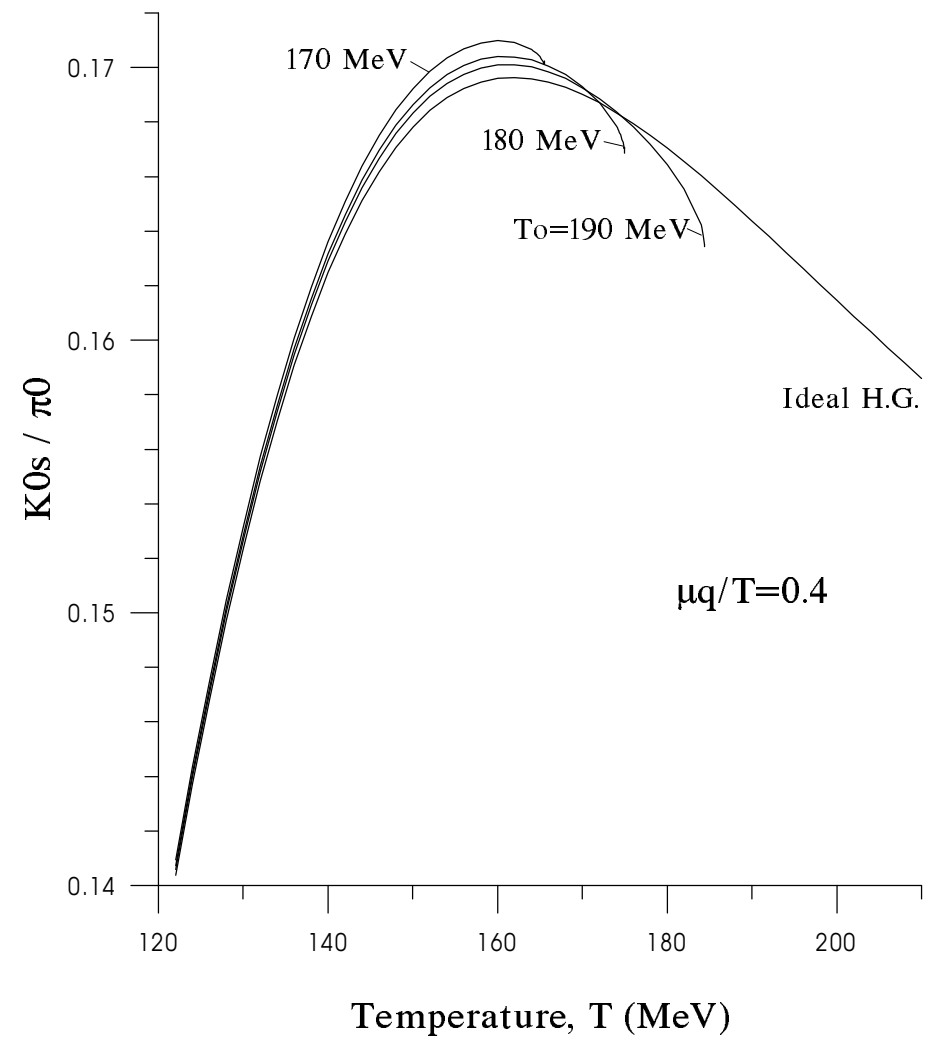


Fig. 12d

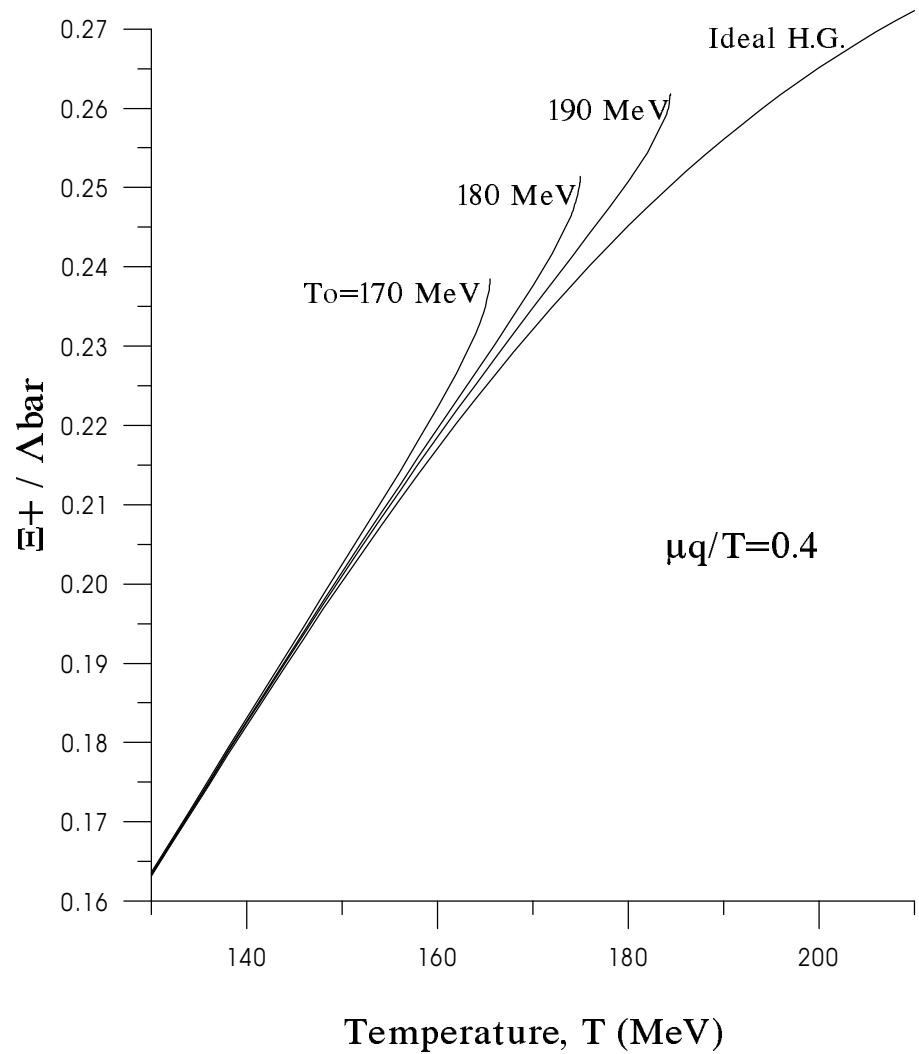


Fig. 12e

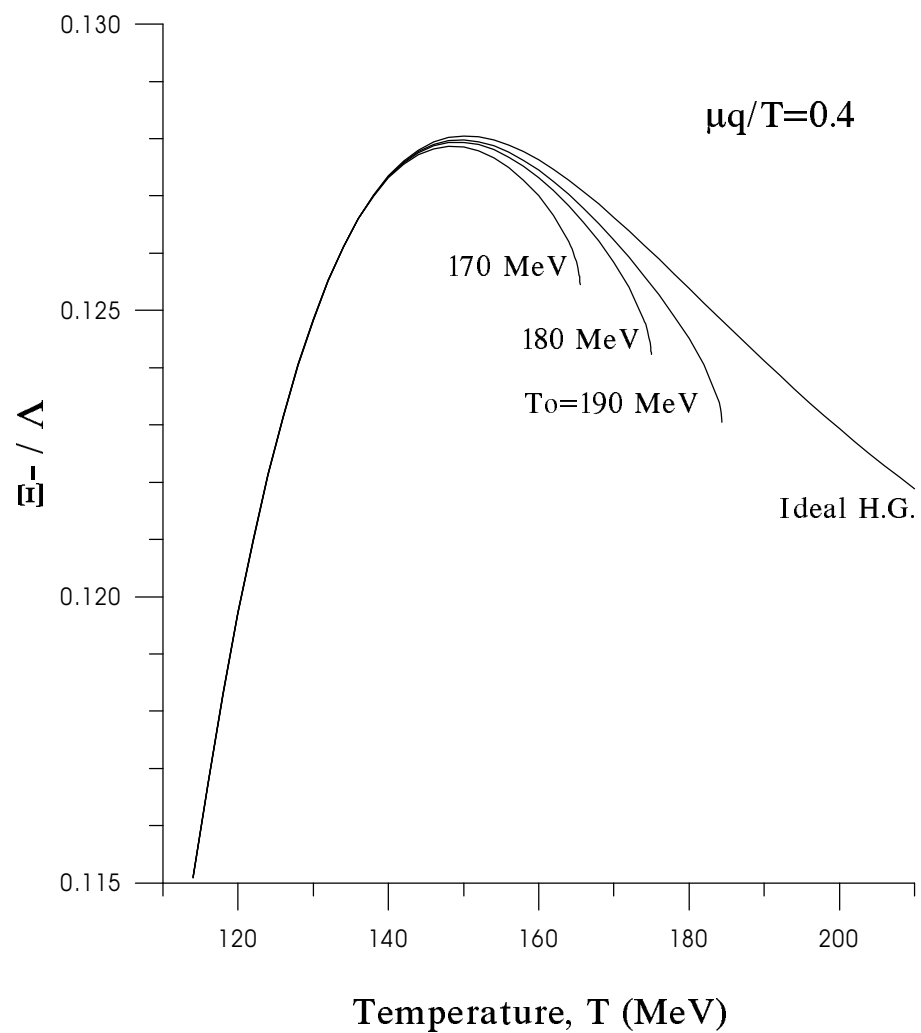


Fig. 12f

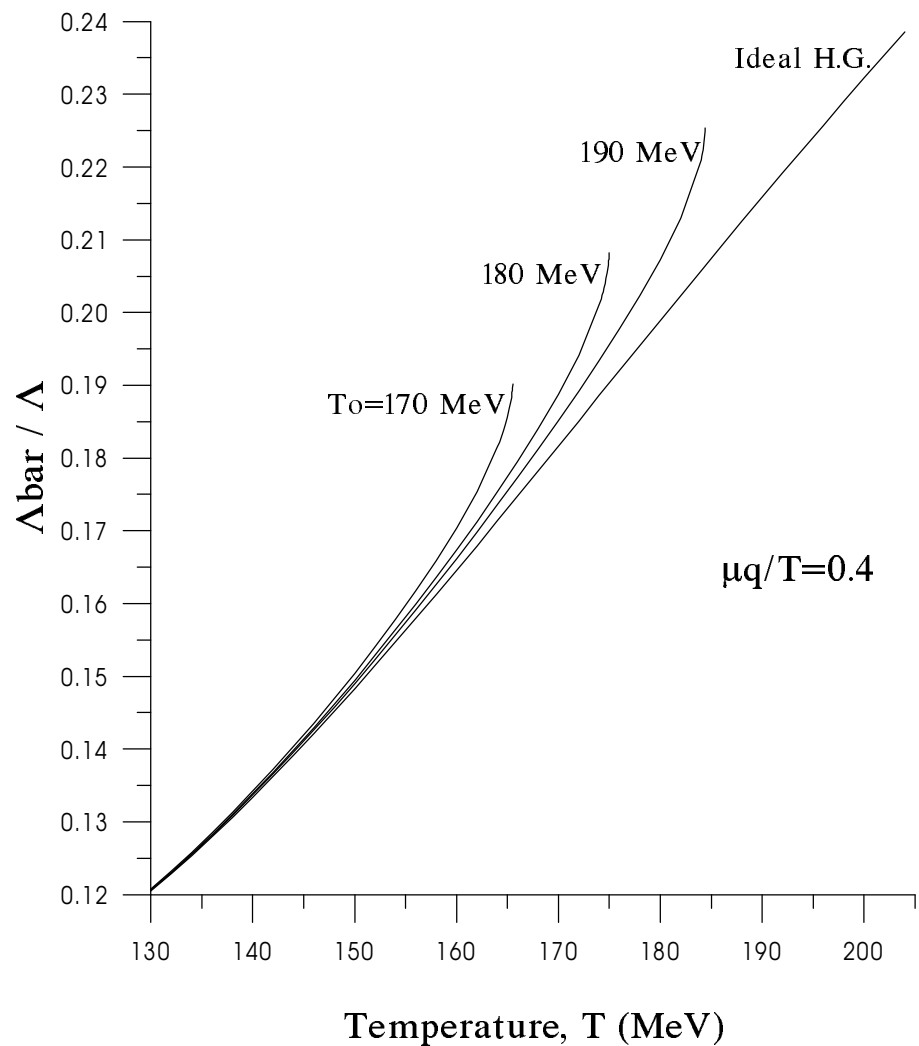


Fig. 12g

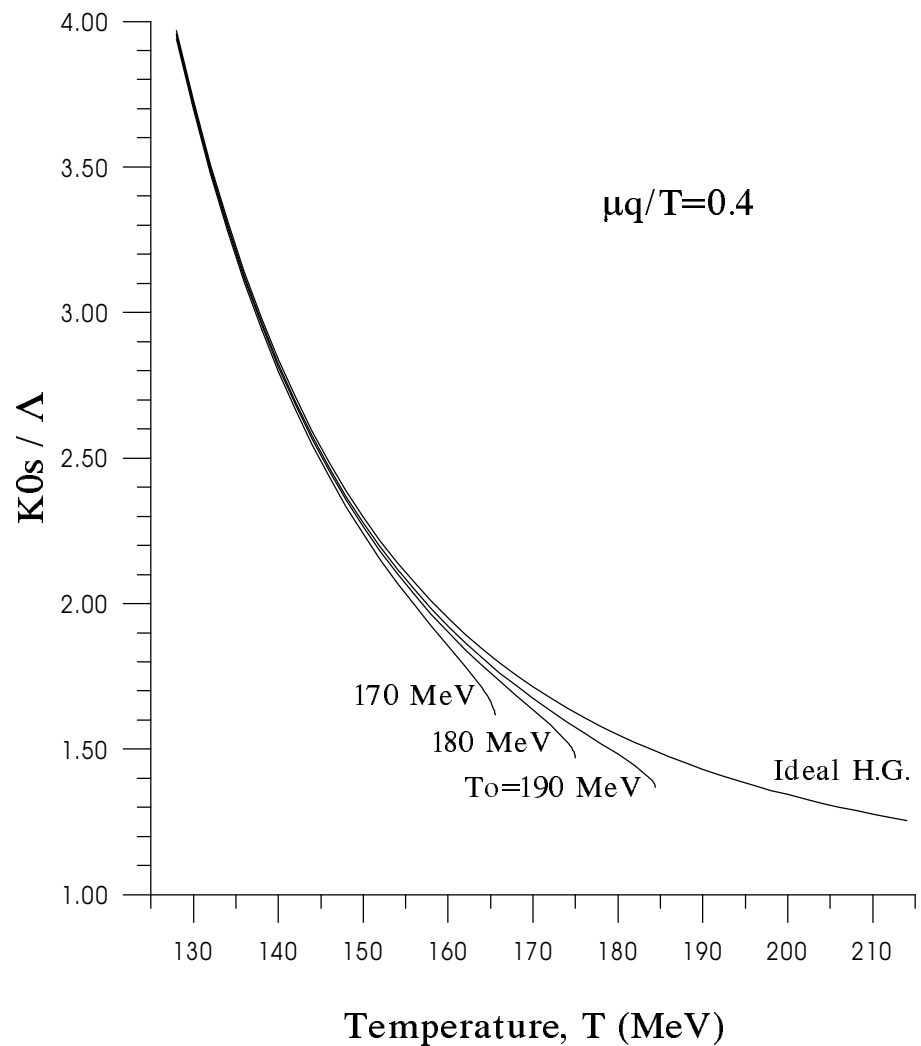


Fig. 12h

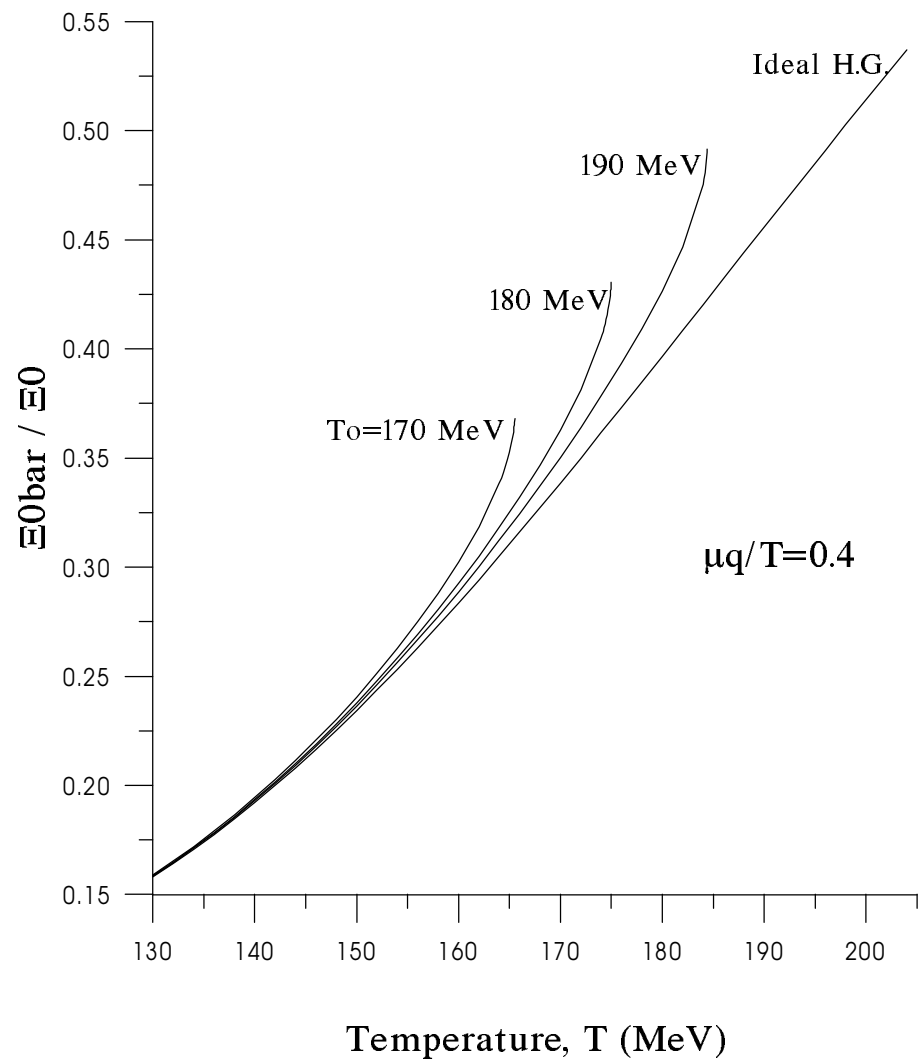


Fig. 12i

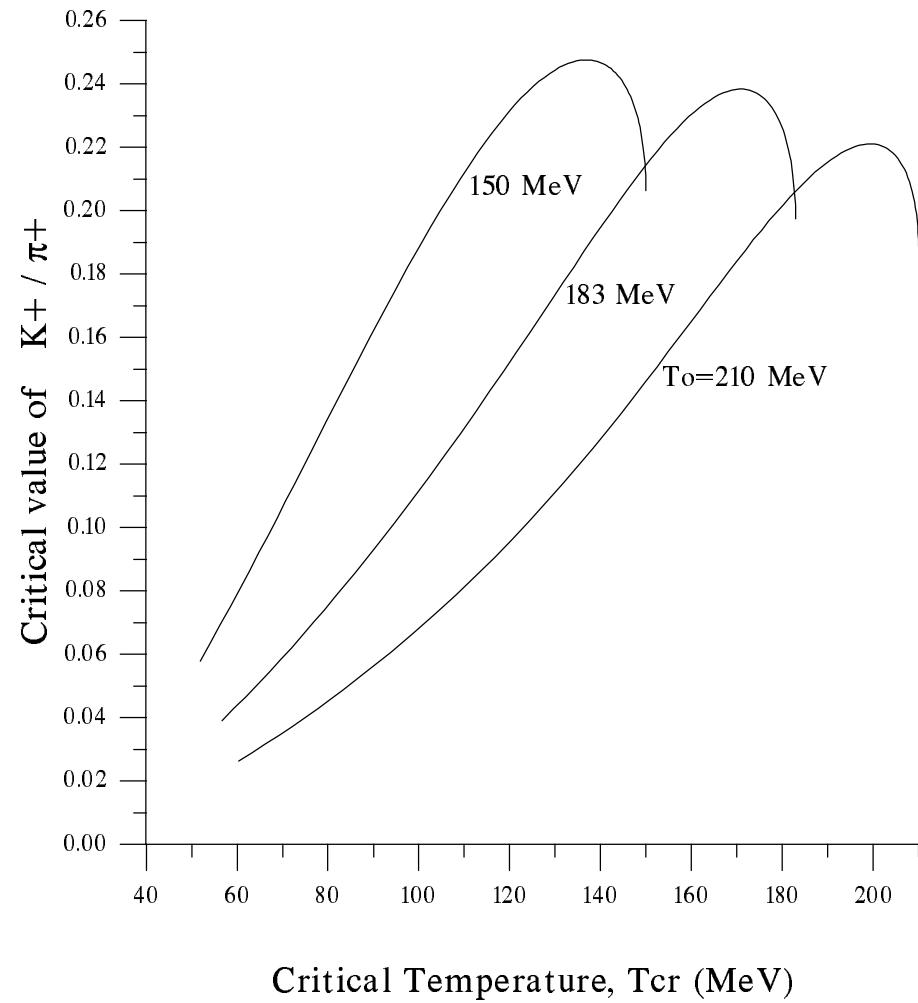


Fig. 13a

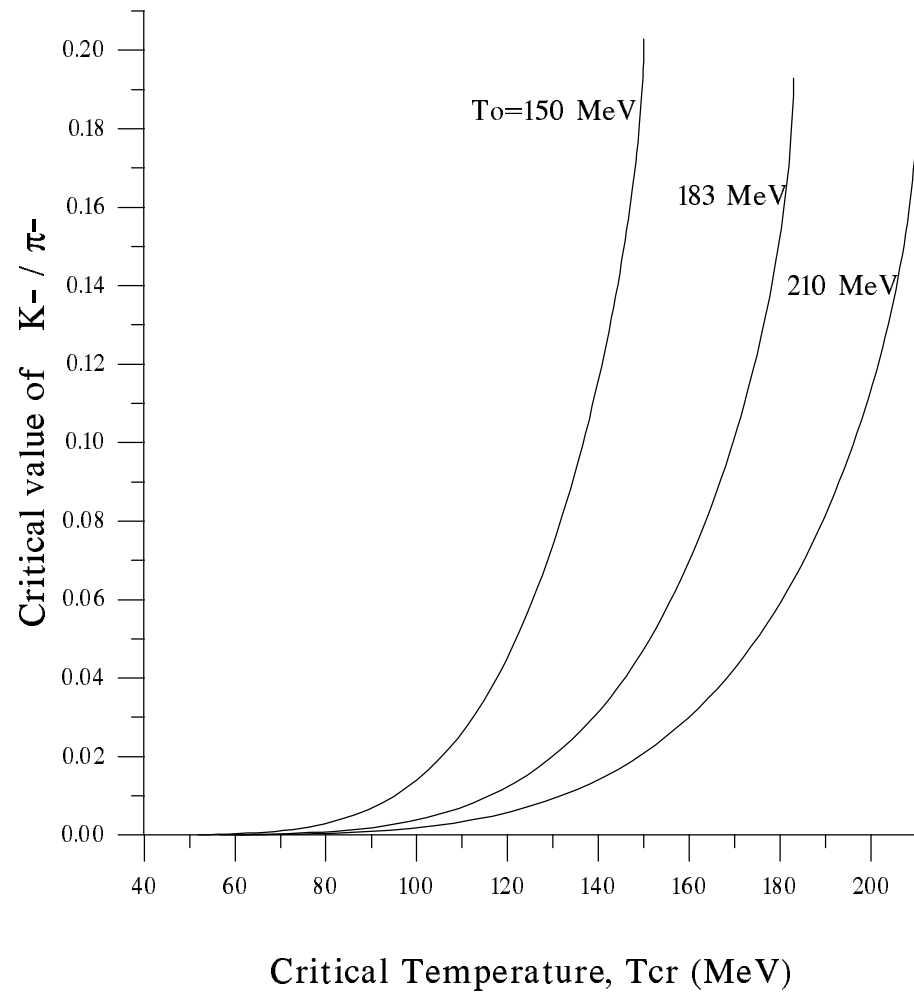


Fig. 13b

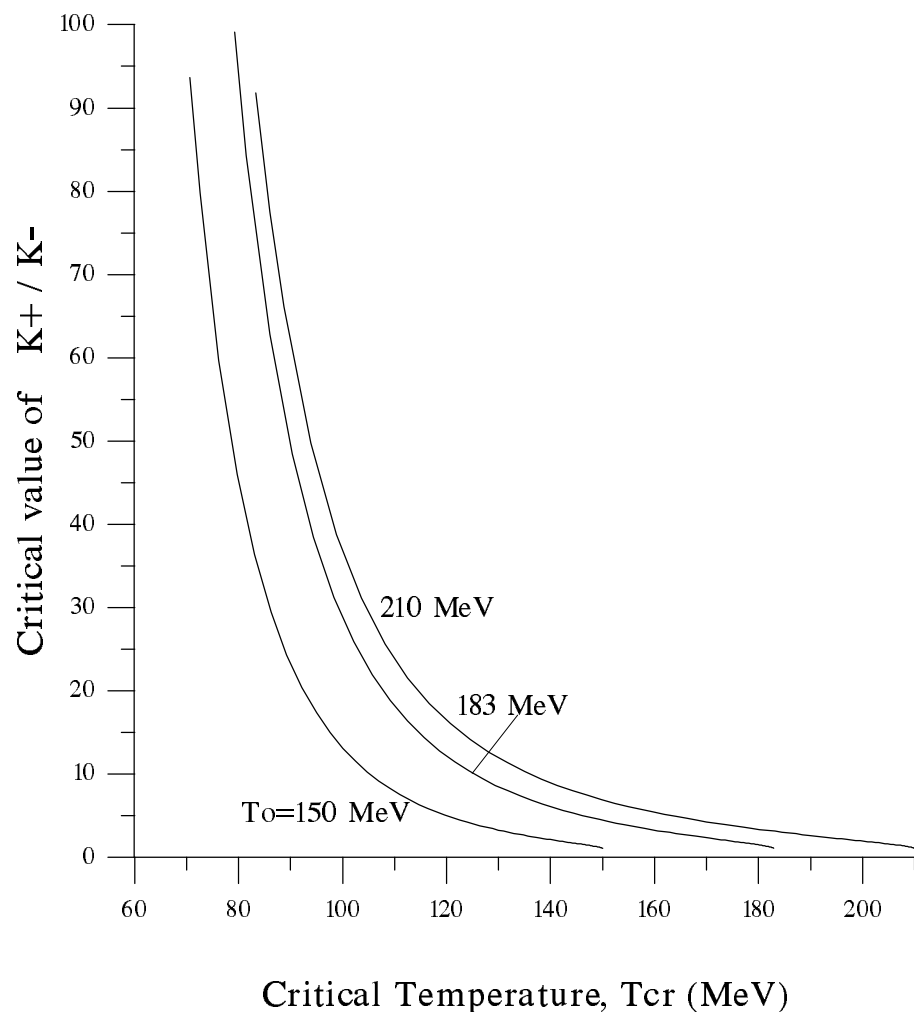


Fig. 13c

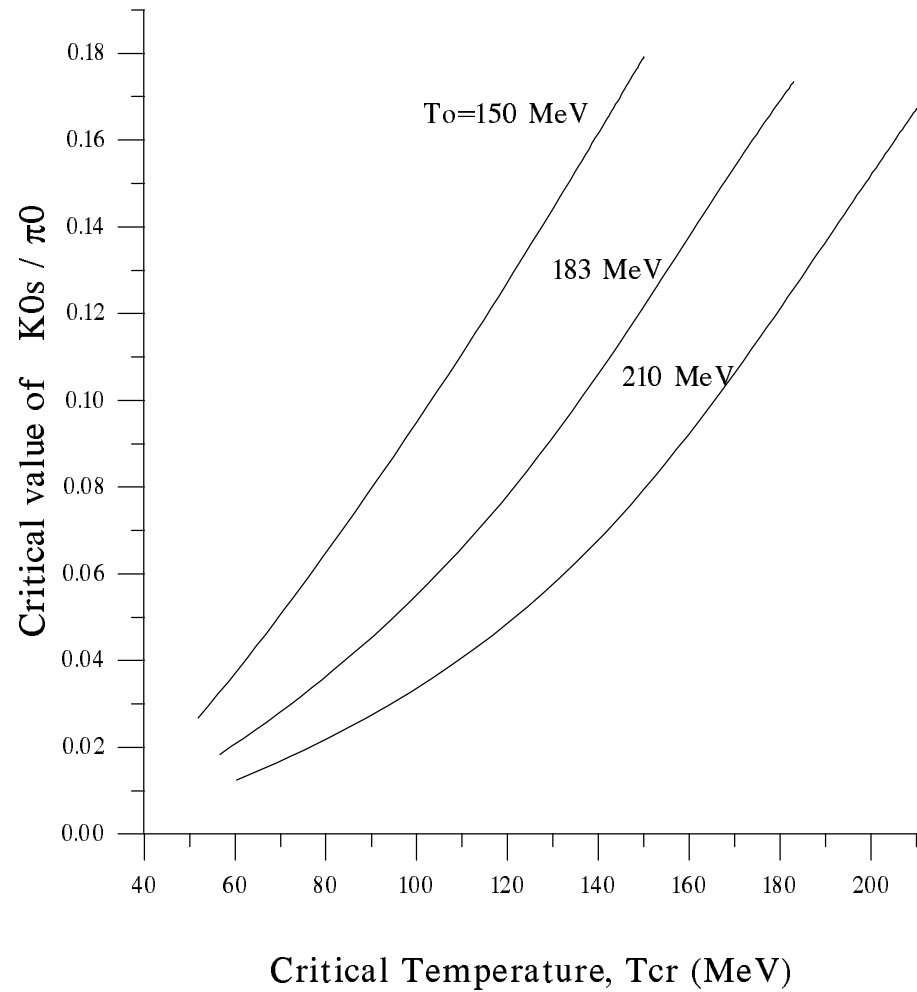


Fig. 13d

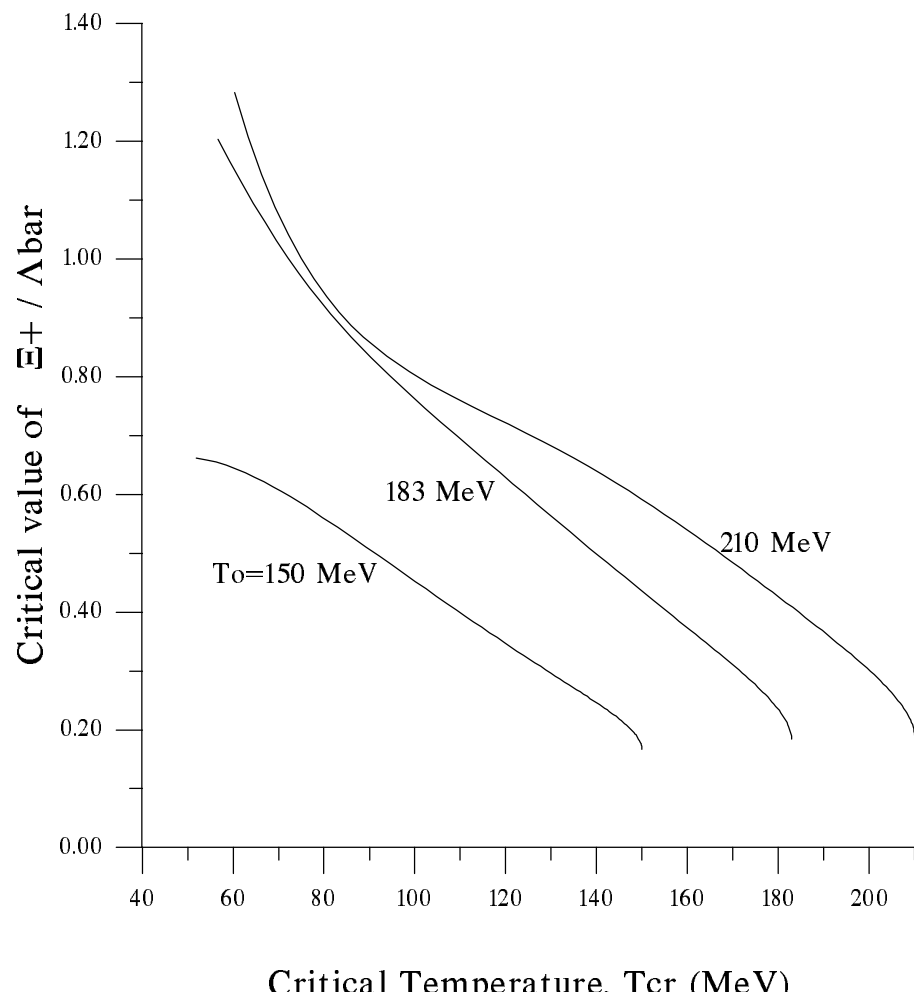


Fig. 13e

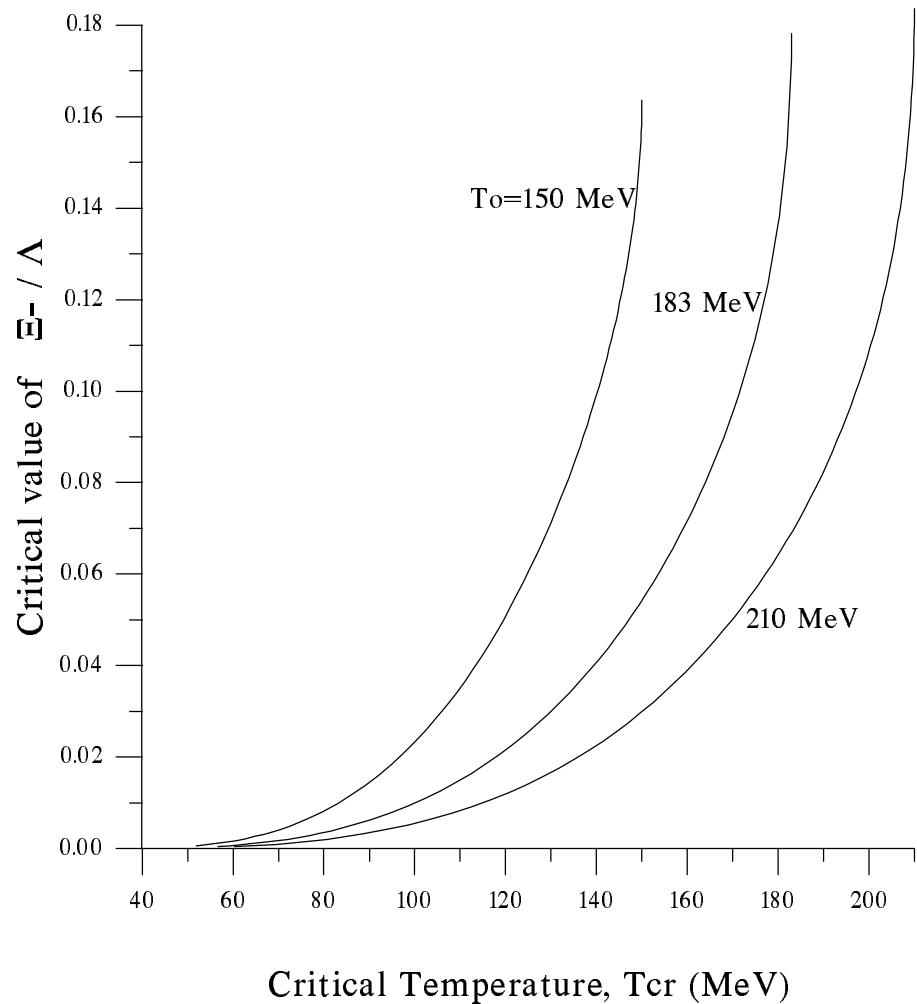


Fig. 13f

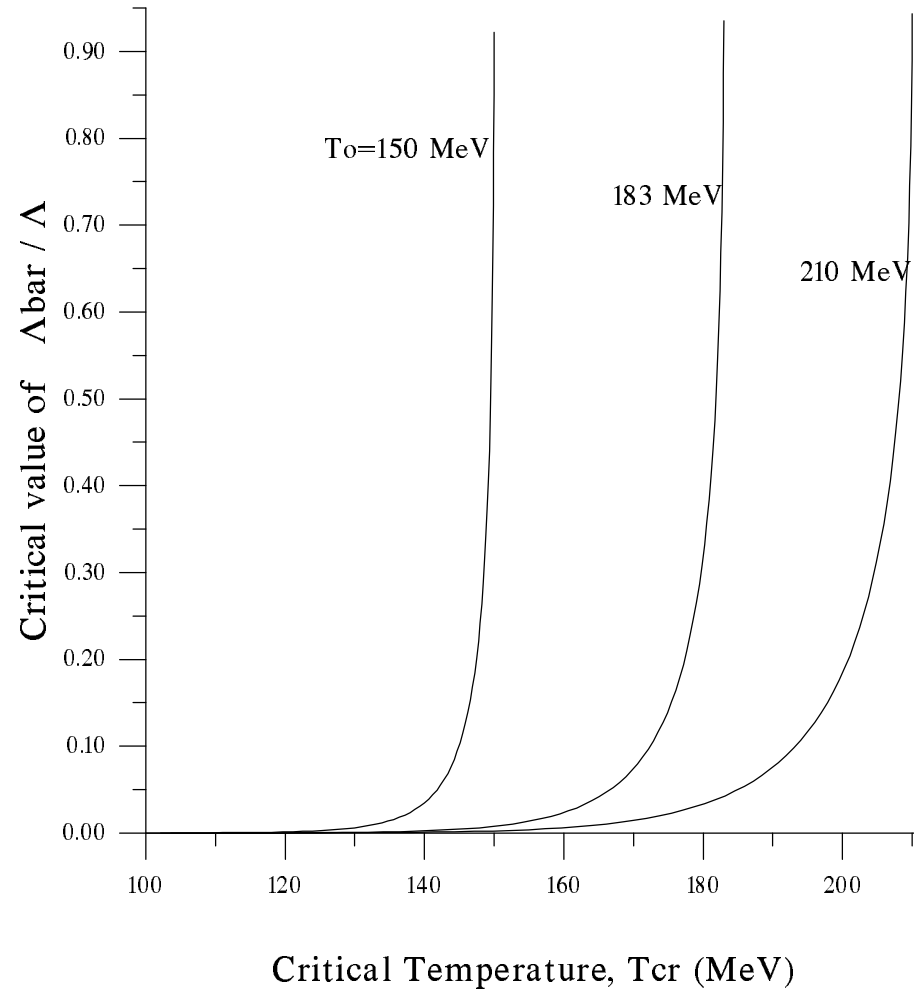


Fig. 13g

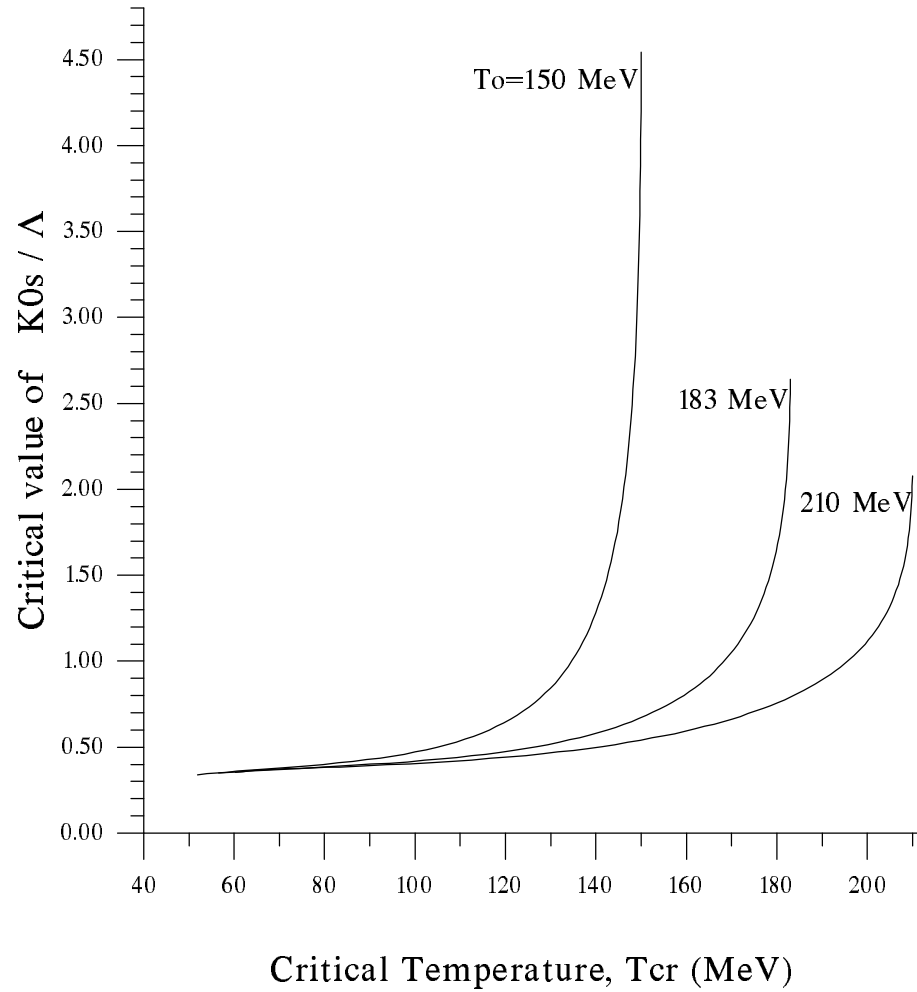


Fig. 13h

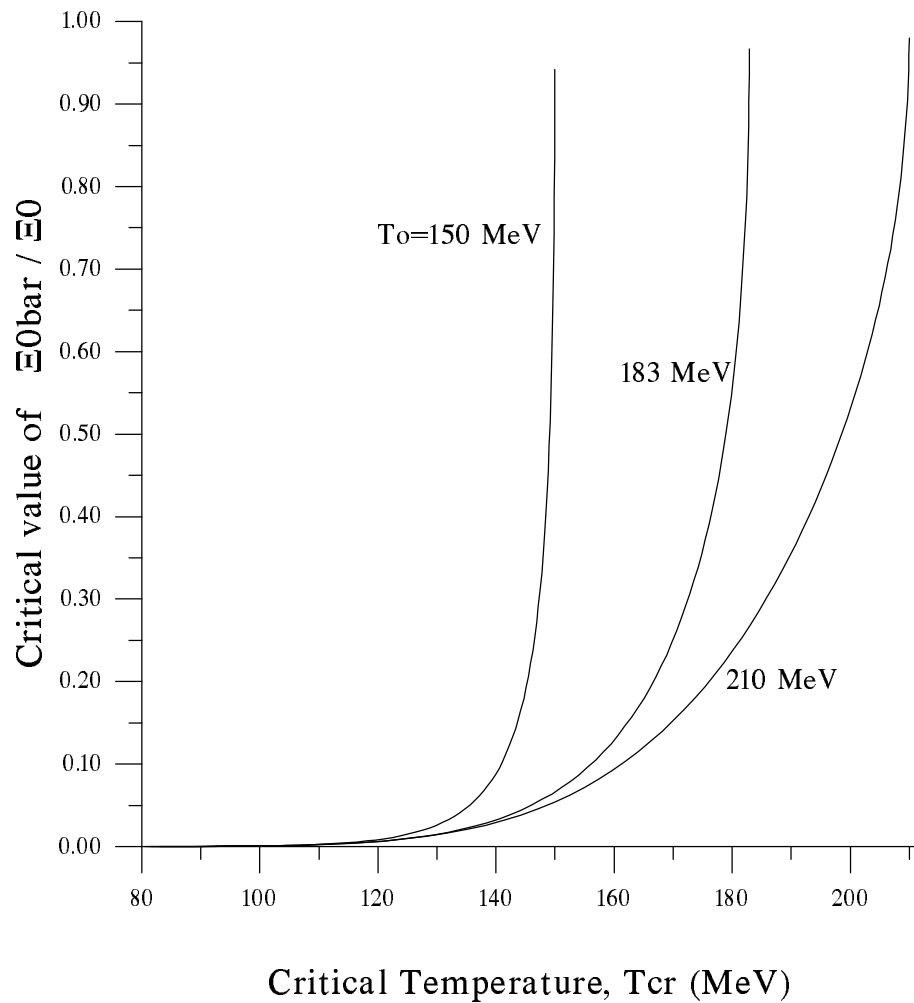


Fig. 13i

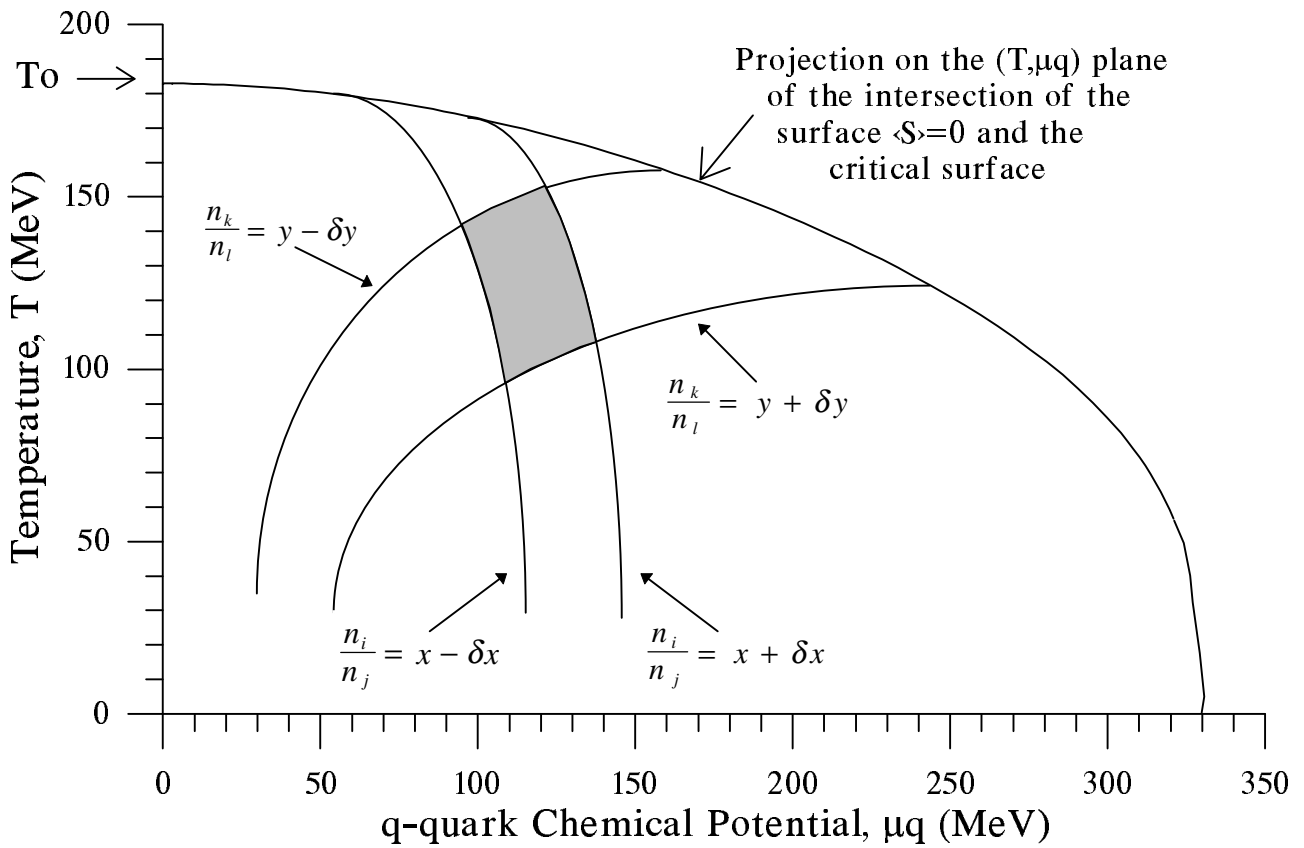


Fig. 14a

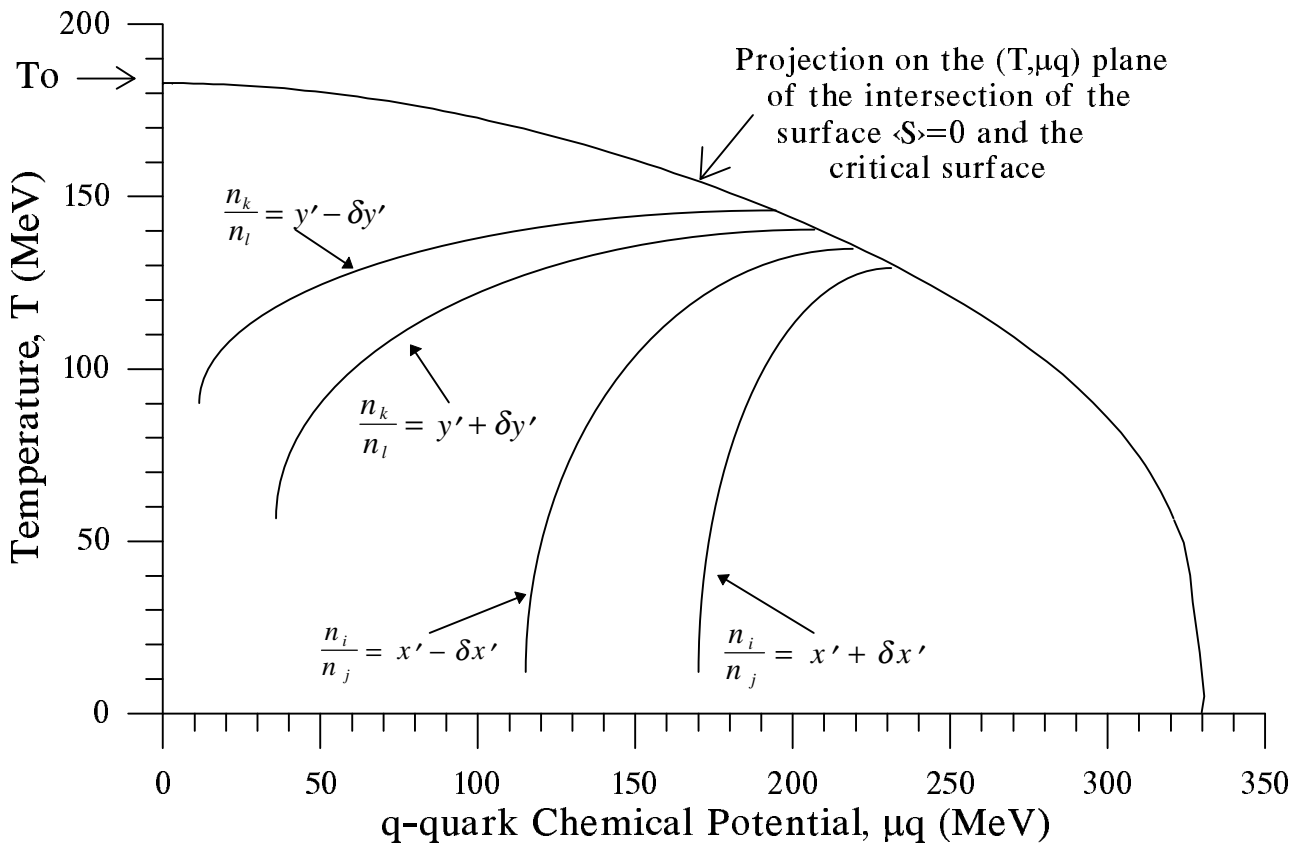


Fig. 14b

